PHYSICAL REVIEW D VOLUME 29, NUMBER 5 1 MARCH 1984

# Nuclear physics and the quark model: Six quarks with chromodynamics

Kim Maltman* and Nathan Isgur
*Department of Physics, University of Toronto, Toronto, Canada M5S 1A7*
(Received 11 May 1983)

We have studied the six-quark system in a nonrelativistic quark model which incorporates some of the features expected from chromodynamics. Using a large basis space which includes color, spin, and orbital excitations, and a Hamiltonian completely determined by previous studies of baryon structure, we derive a number of the features of low-energy nuclear physics. Among our findings are (1) a strong dynamical clustering of the $3u$-$3d$ system into a neutron-proton configuration and (2) an effective nucleon-nucleon potential with a strong repulsive core and an intermediate-range attraction similar to those of semiphenomenological potentials. When supplemented with a reasonable model for one-pion exchange, this effective potential gives a good account of the properties of the deuteron.

Within the last few years it has become clear that QCD is probably the correct theory of the strong interaction and also that it possesses a very complex structure. Given this complexity, it seems unlikely that it will be possible to rigorously deduce its consequences for any but the simplest systems in the near future, so that we must, in the meantime, continue to rely on relatively crude QCD-like models for some insight into many of the phenomena of the hadronic world.

Among the more central issues—both physically and historically—which such models might address is the attempt to derive the properties of simple nuclear systems from QCD. We present here the results of a study[1] of the six-quark system in a QCD-like nonrelativistic quark model[2,3] which has had some success in describing hadronic structure, especially in the baryonic sector most relevant to the present calculation. We find that the major features of the nuclear physics of this system emerge automatically from the model: in the channel with $NN$ quantum numbers we see a dynamical segregration of the six quarks into two three-quark nucleonic clusters and an effective potential between these clusters with a strong repulsive core and an intermediate-range attraction similar to empirical internucleon potentials. When this deduced effective internucleon potential, arising from residual color forces, is used in a hybrid model which incorporates the effects of pion exchange in a consistent way, we find that we can actually account quantitatively for the properties of the simplest nontrivial nucleus, the deuteron.

## I. INTRODUCTION, ORIENTATION, AND FOUNDATIONS

The principal aim of the work described here[1] was to extract predictions for the properties of the six-quark system from a nonrelativistic quark model[2,3] which incorporates some of the features expected from chromodynamics. We stress from the outset that this part of our program was purely deductive: the parameters of the model are all known from studies of baryons so that our results are completely predetermined. Of course we were forced by the complexity of the system in question, with its myriad of spin, color, isospin, and spatial configurations, to make approximations as we proceeded, and one of the main objectives of this paper is to delineate and comment on our procedure so that the reader may decide not only whether the model we have used is appropriate but also whether our results are really consequences of the model.

A subsidiary aim of our work was to reexamine the nature of contributions other than the residual color forces just mentioned to the nucleon-nucleon potential $V_{NN}$. In particular, we believe that models for the meson-exchange contribution to $V_{NN}$ should conform to various qualitative ideas about the nature of QCD. The very success of QCD-like quark models (both potential models like the one we will use here and bag models) supports the picture which has emerged from more fundamental studies, namely, that at short distances QCD is a weakly coupled theory with asymptotically free quark and gluon degrees of freedom, but that at distances of order 1 fm and larger a strong-coupling regime emerges in which color is confined, chiral symmetry is broken, and in which, for example, quark and stringlike degrees of freedom (i.e., collective states) become more appropriate. We will argue on the basis of this picture that the internucleon potential at less than about 2 fm should begin to be free of meson-exchange effects so that the residual color potential we deduce in that region should be a good representation of $V_{NN}$. For internucleon separations much larger than this, quark-pair creation is expected to become important, with the consequences that the deduced residual color potential will be inaccurate and that it must in principle be supplemented by meson-exchange effects. In this complex large-distance regime our program can no longer proceed deductively, but we show that it is very likely, on the basis of the qualitative picture we have just described, that only pion exchange makes a significant contribution to $V_{NN}$. The deuteron, which is rather special in being sensitive to both the short- and long-distance components of $V_{NN}$, fortunately provides a good testing ground for the hybrid model we propose to marry these two regimes, and we show that models which conform qualitatively to our pic-

 

ture will give a reasonable quantitative description of its properties. We return to the role of mesons in Sec. IV, but in the interim we will be concerned solely with the problem of deducing the component of $V_{NN}$ arising from residual quark-quark forces.

The starting point for these calculations is the model Hamiltonian[2,3]

$$H=\sum_{i=1}^{6}\left[m_i+\frac{p_i^2}{2m_i}\right]+\sum_{i<j}(H^{ij}_{\rm conf}+H^{ij}_{\rm hyp})\,, \tag{1}$$

where with $\vec{r}_{ij}=\vec{r}_i-\vec{r}_j$ and

$$S_{ij}=\frac{3\vec{S}_i\cdot\vec{r}_{ij}\vec{S}_j\cdot\vec{r}_{ij}}{r_{ij}^2}-\vec{S}_i\cdot\vec{S}_j\,,$$

$$H^{ij}_{\rm conf}=-[e_0+\tfrac{1}{2}kr_{ij}^2+U(r_{ij})]\frac{\vec{\lambda}_i}{2}\cdot\frac{\vec{\lambda}_j}{2} \tag{2}$$

is the spin-independent part of the quark-quark interaction and

$$H^{ij}_{\rm hyp}=-\frac{\alpha_s}{m_im_j}\left[\frac{8\pi}{3}\vec{S}_i\cdot\vec{S}_j\delta^3(\vec{r}_{ij})+\frac{1}{r_{ij}^3}S_{ij}\right]\frac{\vec{\lambda}_i}{2}\cdot\frac{\vec{\lambda}_j}{2} \tag{3}$$

is the hyperfine interaction responsible, among other things, for the $\Delta$-$N$ splitting. Here $e_0$ is a constant which plays no role in the energy differences which concern us and $U$ is an anharmonicity, to be discussed below, which represents the expected strong Coulomb-type interaction of QCD and also other departures from the harmonic limit.[4] For application to a system as complicated as the one being studied here, the extreme simplicity of this model is a great virtue. The model is chosen, however, primarily for its success in describing hadronic spectra and dynamics, especially in the baryonic sector where we most require it to be accurate. Being a model, it is, of course, not without its weaknesses and before proceeding we comment on these weaknesses and their effect on the reliability of our calculations:

(i) The neglect of spin-orbit terms in Eq. (1) is allowed since the data on baryon resonances require that spin-orbit effects be small, although the reason for their suppression is not well understood.[2,3,5] However, given that the model fits baryon spectroscopy and decays, the influence of this uncertainty on our conclusions should be negligible.

(ii) Since we are mainly concerned with the properties of the six-quark system *relative* to those of two separated three-quark clusters, many sources of error in the calculation—nonrelativistic approximations among them—are reduced.

(iii) The two-body confinement potential [Eq. (2)][6] can be criticized on several grounds. First, it is known to lead to a long-range van der Waals—type force between nucleons whose strength is incompatible with experiment.[7] Note, however, that such long-range forces arise only in the approximation that the confinement potential between two colored objects in an overall color singlet is allowed to grow indefinitely, undamped by $q\bar{q}$ pair creation. Thus, although one must be cautious (as indeed we are: see below) about the possible presence of spurious long-range effects in the calculation, we do not believe this to be a fundamental obstacle to employing potentials of this form. A second criticism of (2) is that it leads to various pathologies (e.g., spectra unbounded from below) in multiquark systems.[7] We believe that this also is not a fundamental problem since no pathologies appear in the physical (i.e., overall color-singlet) sector of the theory[8] where, for example, one can easily show that (2) is bounded from below for harmonic forces. Finally one can criticize (2) for being too limited to comply with the requirements of local gauge invariance for large quark separations where stringlike degrees of freedom are required.[9] While there are some indications from string models that (2) may be a reasonable approximation for low-lying states,[10] such a correspondence remains to be proved. In the interim, however, we believe these results support our opinion that (2) is a phenomenologically acceptable representation of confinement.

(iv) The radial dependences of the potentials in (2) and (3) are oversimplifications. More suitable, for example, would be the sum of a linear and a Coulomb-type term in (2), but of course such a potential would be considerably more difficult to use. Since the baryon spectrum is well reproduced by this Hamiltonian up to masses corresponding to interquark distances as large as those for which we plan to take (1) seriously, this seems a sensible simplification. In perturbation theory, the baryon spectrum up to $N=2$ is actually independent of the form of $U$,[4] so we have taken $U(r_{ij})=-w\delta^3(\vec{r}_{ij})$ to further simplify the calculations. (Incidentally, although strictly speaking the $\delta$ function is an illegal operator for the Schrödinger equation, its appearance here and in the contact piece of the hyperfine interaction poses no problem, for reasons to be elaborated below. Moreover, since in our calculations those interactions will be smeared over clusters, our results are quite insensitive to the specific radial forms chosen.)

As already stressed, the parameters of the model are all known from previous studies of baryon spectroscopy. They are given in Table I in the combinations in which they naturally occur in this calculation.

## II. A HISTORICAL INTERLUDE

Before describing our method and results, we will briefly review some previous work in the area. Attempts to understand the nucleon-nucleon force in the context of the quark model have, in fact, a long history.[12–21] The modern attempts date from the investigations of Liberman[13] (in a potential model) and DeTar[14] (in a bag model), though it is now believed that their methods were inadequate.[15] Among the important problems noted in Ref. 15 was the neglect of states with non-nucleonic spin and color configurations as well as those of low spatial symmetry. The latter, in particular, were known to be of potential importance since the antisymmetry of the six-quark state requires that such states be coupled to the higher color-spin symmetries favored by the color-magnetic interaction. Harvey,[16] performing a calculation of the Liberman type [but with a more realistic Hamiltonian similar to (1)], showed that, indeed, both the mixing of $\Delta\Delta$ and of a hidden color state into the two-nucleon wave function and the inclusion of states of lower spatial

TABLE I. Input parameters to the calculation of the $NN$ effective potential.

| Parameter | Value[a] | Comment |
|---|---|---|
| $m$ | 330 MeV | The nonstrange constituent quark mass |
| $\alpha$ | 320 MeV | The nonstrange cluster parameter |
| $\frac{3}{2}k\alpha^{-2}$ | 198 MeV | Follow from the SU(6) multiplet pattern up to $N=2$ |
| $\frac{w\alpha^3}{(2\pi)^{3/2}}$ | 176 MeV | |
| $\frac{8\pi\alpha_S\alpha^3}{3(2\pi)^{3/2}m^2}$ | 260 MeV | Related to the $\Delta$-$N$ splitting |

[a]These values are all given in or obtainable from Ref. 2 except for the last entry which is given there as having the value 300 MeV. More recent studies taking into account various small effects (see Ref. 11) have revised the best value of this parameter to that quoted here.

symmetry had dramatic effects: the putative repulsive core was transformed into a weak attraction. While we will see (as have others: see, e.g., Harvey in Ref. 20) that an adiabatic approximation is not viable for this system, the basic point of Harvey's work, that configuration mixing can be very important, still remains very much in force. It should be pointed out in passing that not all the possible states which have unexcited clusters and can be coupled to the two-nucleon channel have been considered in Harvey's calculation. This is because only states with the same SU(4) spin-isospin quantum numbers as the input channel were used. This is, of course, not justified if the forces are, as indeed they are here, strongly spin dependent. We will return to this point later.

Most of the very recent work done on the two-nucleon force has followed the line of direct descent from early nuclear-physics-inspired speculations and employed either the resonating-group or generator-coordinate methods developed by Wheeler and his collaborators.[22] Beginning with the work of Warke and Shanker,[18] such calculations have been steadily improved through the use of more realistic potentials and the inclusion of a larger number of input channels.[19,20] The results, in all cases, show persistent negative $S$-wave phase shifts, thus implying the existence of a repulsive core (a core whose nature is, in fact, consistent with what we will find below), and demonstrating the inadequacy of the adiabatic approximation (a result on which we are also in agreement).

While a consensus on these last two points may have been reached by previous workers (see, however, Ref. 21), a number of problems still remain. While other calculations have considered at most Harvey's three channels, Rosina *et al.*[19] find indications that the inclusion of all six possible $S$-wave cluster states (which we use) may be important. The calculations done to date have also, so far as we are aware, assumed that any spatial excitations of importance must occur in the intercluster coordinate. This prejudice, which may hark back to previous experiences with such calculations in nuclear physics, is no longer justified *a priori* in the present case where the color degree of freedom may intercede. We have included such effects in our calculation and find that they are indeed significant: they appear to be responsible for the attractive part of the internucleon potential.

## III. METHODS AND RESULTS FOR THE RESIDUAL COLOR INTERACTION

While the resonating-group method has the advantage of working directly with the measurable phase shifts, the fact that it involves solving a set of coupled integrodifferential equations soon leads to intractable numerical difficulties as the number of coupled states is increased. Since it is our aim to include in the calculation all six $S$-wave cluster states, as well as more than a hundred states with excited clusters, plus the $NN$ relative $D$-wave state, plus, eventually, the effects of meson exchange, such a method of calculation is not suitable. For this reason we have chosen the much more modest approach of performing a bound-state variational calculation for the ground state of the six-quark system. Despite being more modest, this approach in fact allows us to examine several interesting aspects of the problem rather directly:

(1) We are able, simply by decomposing our states, to examine the proposition (obviously central to nuclear physics as we know it) that, in channels with $NN$ quantum numbers, the six-quark system is well approximated by two nucleonic clusters.

(2) Once given that a nucleon-nucleon interpretation indeed arises from (1), we are able to extract a bound-state-equivalent effective potential from our variational intercluster wave function and examine it for the presence or absence of the dominant features of empirically determined potentials, namely, the intermediate attractive region and the repulsive core.

(3) Although uncertainties which we discuss below make our results less quantitative than we might like, we are able to calculate various static properties of the $NN$ ground states, such as binding energies, charge radii, etc.

On the other hand, if we wish to compare our results to experimental phase shifts we will have to assume an equivalence of our bound-state effective potential with the phase-shift effective potential.

As we have already stated, the main reason for choosing the ground-state variational calculation over the resonating-group method is that by making this choice we have been able to work with a far larger space of states than has heretofore been possible. We have found it possible to decrease our effort even further by the following simple tactic: by specializing to the case of three $u$ and three $d$ quarks and allowing isospin to emerge dynamically, we have been able to construct properly antisymmetrized six-quark states using the irreducible representations and Clebsch-Gordan coefficients of $S_3^u \times S_3^d$ (as given in Appendix A) rather than those of $S_6$. This greatly simplifies the evaluation of matrix elements, although, since isospin is not manifest, it forces us to diagonalize larger Hamiltonian matrices than we would have had in the isospin basis. This does not prove to be a problem. The equivalence of the two approaches is demonstrated in Ref. 1.

Given the complicated structure of the six-quark system

it is important to choose spatial coordinates which make a physical interpretation of the states obtained as simple as possible. In this regard we have been guided by the success of standard nuclear physics (especially in light of the results of Ref. 23) and chosen as natural relative coordinates the internal coordinates of two three-quark clusters and the corresponding intercluster coordinate. Of course, if the dynamics of the calculation are such that three-quark clustering does not dominate the resulting state, this will be reflected in large exchange overlaps and an inability to interpret the intercluster wave functions in a probabilistic manner. (The situation is analogous to cluster calculations in nuclear physics where, for example, after antisymmetrization, the $d+\alpha$ and $t+{}^3\mathrm{He}$ description of the low-lying state of ${}^6\mathrm{Li}$ are equivalent[24].)

The calculation then proceeds in three phases. In the first we restrict ourselves to states which are the appropriately antisymmetrized versions of two three-quark $S$-wave clusters in a relative $S$ wave, but with all possible spin and color excitations. In the isospin basis these states are $N\frac{1}{2}N\frac{1}{2}$, $\Delta\frac{3}{2}\Delta\frac{3}{2}$, $N_c\frac{3}{2}N_c\frac{3}{2}$, $N_c\frac{1}{2}N_c\frac{1}{2}$, $N_c\frac{3}{2}N_c\frac{1}{2}$, and $\Delta_c\frac{1}{2}\Delta_c\frac{1}{2}$ in the $I=0$, $J=1$ channel and $N\frac{1}{2}N\frac{1}{2}$, $\Delta\frac{3}{2}\Delta\frac{3}{2}$, $N_c\frac{3}{2}N_c\frac{3}{2}$, $N_c\frac{1}{2}N_c\frac{1}{2}$, $\Delta_c\frac{1}{2}\Delta_c\frac{1}{2}$, and $\Delta_c\frac{1}{2}N_c\frac{1}{2}$ in the $I=1$, $J=0$ channel. (The notation here gives the isospin and spin of the clusters as $I_1S_1I_2S_2$; the subscript $c$ denotes a cluster in a color-octet state. The phase-I basis states in the $S_3^u\times S_3^d$ basis are derived in Appendix B. There are 15 $I_3=0$ states with $J=1$ and 9 with $J=0$; for the equivalent isospin decomposition, which leads to the identification of the above-mentioned states, see Ref. 1.) The spatial wave function of each three-quark cluster is taken to be that of the nucleon ground state,[2] e.g., for the cluster 123

$$\phi(\vec{\rho}_{123},\vec{\lambda}_{123})=\frac{\alpha^3}{\pi^{3/2}}\exp[-\tfrac{1}{2}\alpha^2(\rho_{123}{}^2+\lambda_{123}{}^2)] \tag{4}$$

with

$$\vec{\rho}_{123}=\frac{1}{\sqrt{2}}(\vec{r}_1-\vec{r}_2)\,, \tag{5}$$

$$\vec{\lambda}_{123}=\frac{1}{\sqrt{6}}(\vec{r}_1+\vec{r}_2-2\vec{r}_3)\,, \tag{6}$$

while the intercluster wave function (common to all phase-I basis states) is expressed as

$$\Psi(\vec{r})\sim\sum_{i=1}^{i_{\max}}\xi_i\exp(-\tfrac{1}{2}\beta_i{}^2r^2)\,, \tag{7}$$

where $\xi_i,\beta_i$ are variational parameters and $\vec{r}$ is the intercluster separation. The form (7) was chosen to facilitate calculations, but even so we found the process of minimizing energies in $\beta_i,\xi_i$ unwieldy if we went beyond three terms. The cluster size $\alpha$ in (4) was not allowed to vary from the value used in baryon spectroscopy, as given in Table I. This was done not only to keep the number of variational parameters to a minimum but also to allow an important technical simplification: if $\alpha$ is treated variationally then the simple form used for the spatial dependence of the hyperfine and $U$ potentials must be modified. This would require not only the evaluation of more difficult matrix elements but, far more importantly, the reworking of baryon spectroscopy and decay analyses. We will comment in the concluding section on the possibility of including $\alpha$ as a variational parameter; we will also argue there that, in view of some simple checks we have made, the procedure of holding $\alpha$ constant should not affect the nature of our conclusions.

Phase I of our calculation was carried out by taking matrix elements of color, spin, and spatial operators in the appropriately antisymmetrized basis of Appendix B. The matrices required in these sectors are given in Appendices C, D, and E, respectively. The Hamiltonian matrix in both spin channels was then constructed (Appendix F gives the kinetic matrix elements required to complete the matrix) and diagonalized for various choices of $\beta_i,\xi_i$ in (7) until a variational minimum was found. [In the event that no bound state was found the Hamiltonian (1) was supplemented by an artificial weak harmonic attraction which allowed one to extract information on the short-range behavior of the system.] In both the $J=0$ and $J=1$ sectors the resulting intercluster wave function was strongly suppressed at $r=0$ and the system showed an almost complete dynamical clustering into the neutron-plus-proton configuration (as measured by small admixtures of other color, spin, and isospin components and by extremely small exchange integrals even within the $np$ component). The phase-I bound-state effective $np$ potential

$$V_{\mathrm{eff}}\equiv E+\frac{\nabla^2\Psi(r)}{M_N\Psi(r)} \tag{8}$$

was characterized by a large repulsive core and weak ($\sim 5$ MeV) intermediate range attraction, with the ${}^1S_0$ potential more repulsive for $r\lesssim 1$ fm and less attractive for $r\gtrsim 1$ fm than the ${}^3S_1$ potential. [Note that there are possible ambiguities associated with the definition (8); see Sec. V.]

In phase-II of our calculation we expanded the basis space to include the most important states with up to two units of orbital excitation. While it would in principle be possible to construct new antisymmetrized states analogous to those of Appendix B based on such states and to include them in a generalization of the phase-I calculation, such a program would be difficult to actually execute. Fortunately, the results of phase I provide a natural and reasonable approximation scheme for including the effects of such states: given the dynamically enforced dominance of the $np$ component and the smallness of the intercluster overlap integrals, we added to our calculation those matrix elements connecting the new spatially excited states directly to the $np$ system, and evaluated these matrix elements only to leading order in the small exchange overlap integrals. We also added the $np$ $D$-wave state which, due to its potential near degeneracy in energy, can be significantly mixed despite the exchange suppression. With these approximations, the new states entering the calculation were four states composed of internally excited color-octet $P$-wave clusters coupled to the $np$ system by the spin-singlet color-dependent potentials, and 109 states (one of which is the ${}^3D_1$ $np$ state) coupled by the tensor interaction. Discussion of the enumeration of these states and the evaluation of the required matrix elements is relegated to Appendices G, H, and I. We note that the

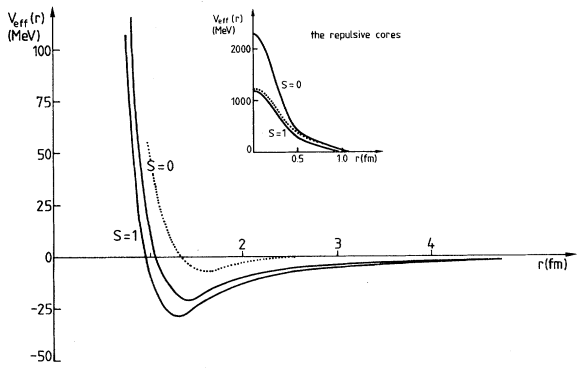


FIG. 1. The effective nucleon-nucleon potential from residual quark forces in the $^3S_1$ and $^1S_0$ channels (solid curves); for comparison the "phase-I" $^3S_1$ potential is also shown (dotted curve).

four $P$-wave color-octet cluster states are the ones that eventually give rise to the spurious long-range tail of the van der Waals force. Nevertheless, their effects in the region corresponding to that in which the interquark potential is well grounded (i.e., $r \lesssim 2.5$ fm) must be taken into account. (As we have remarked above, in a more realistic treatment the long-range van der Waals potential would be damped by $q\bar{q}$ pair creation.) To complete phase II of our calculation, the ground-state energy in each sector was reminimized in the old $\beta_i, \xi_i$ as well as with respect to independent variations of the intercluster wave functions of the new states. While the tensor interaction proved to have an almost negligible effect, admitting spatially excited clusters significantly increased both the depth of the intermediate range attraction in the $S$-wave potentials and their splitting, while producing only small changes in the repulsive cores. The resulting phase-II effective nucleon-nucleon potentials associated purely with residual quark forces are shown in Fig. 1. They are quite similar to potentials commonly used in low-energy nuclear physics.[25] The phase-I $^3S_1$ potential is also shown for comparison.

We have argued earlier, in qualitative terms, that residual quark forces should both dominate $V_{NN}$ and be reliably calculable for separations $r \lesssim 2$ fm. For distances much greater than this, however, we know that the naive interquark potential will be screened by $q\bar{q}$ pair creation and that, as a result, meson exchange will provide the dominant contribution to $V_{NN}$. We will return to a discussion of the spurious long-range van der Waals potential below, but first let us concentrate on the role of meson exchange in the nucleon-nucleon potential.

## IV. MESONS IN THE INTERNUCLEON POTENTIAL

Given that mesons and nucleons have radii ($r_M$ and $r_N$, respectively) which characterize the spatial extent of their quark substructure, it is difficult to imagine—in the most naive geometrical terms—that meson exchange can be very relevant in the two-nucleon system for distances $r \lesssim 2r_N + 2r_M$ (see Fig. 2). For pions, this distance is $\sim 2$ fm, and for excited mesons even larger so that it seems to us probable that only residual quark forces contribute to the internucleon potential for $r \lesssim 1.5$—$2.0$ fm. While Fig. 2 is based on a picture of the transition from the perturbative to confinement regimes of QCD that is consistent with both our model and with fundamental studies, it is obviously a picture that we can at best implement semiquantitatively. Fortunately, the repulsive core tends to overwhelm any other effects for $r \lesssim 1$ fm and for $r \gtrsim 2$ fm mesons effects tend to be small so that in the end our results are not too sensitive to the imprecision of this picture.

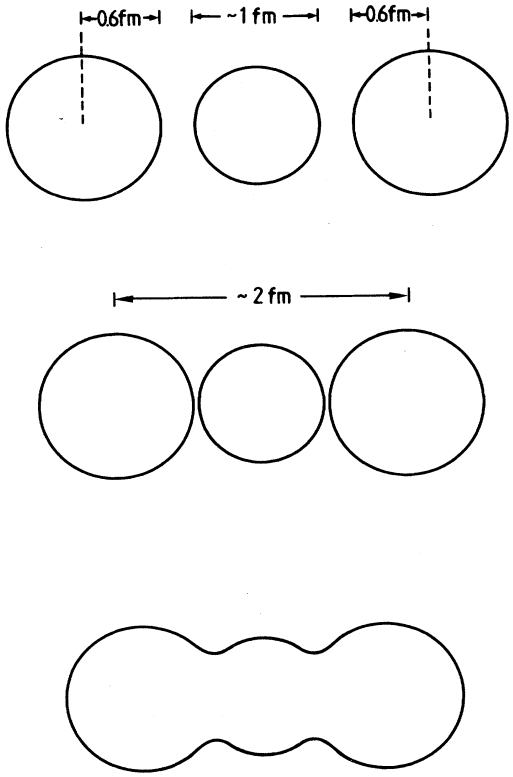


FIG. 2. A cartoon illustrating in naive geometrical terms that for $r \lesssim 2r_N + 2r_M$ meson exchange is unlikely to be appropriate to the description of the internucleon potential.

We first point out that, of all mesons, only the pion is likely to play a significant role. This is illustrated in Table II where the Yukawa suppression factors $e^{-mr}$ of some low-lying mesons, together with their expected contributions to $V_{NN}$ at $r = 2r_N + 2r_M$, are displayed. These results lead us to advocate a picture in which the long-range part of the $NN$ potential is dominated by pion exchange and the short-range part by residual quark forces.[26]

In the third and final phase of the calculation we have implemented this semiquantitative hybrid picture by adding to our phase-II effective potential a modified one-pion-exchange (OPE) potential obtained by suppressing the pion field (and thereby the resulting potential) within the nucleons. Our procedure is described in Appendix J. The resulting potential produces only small changes in the diagonal $^3S_1$ and $^1S_0$ potentials of Fig. 1, but leads to a significant $^3S_1$-$^3D_1$ mixing through its tensor part (see

TABLE II. The role of mesons in $V_{NN}$. Here $r_N$ is the quark-model nucleon radius of 0.6 fm and $r_M$ the quark-model meson radii which we estimate to be $r_\pi \simeq r_\eta \simeq r_{\eta'} \simeq 0.35$ fm, $r_\rho \simeq r_\omega \simeq 0.5$ fm, $r_P \simeq 0.7$ fm, and $r_D \simeq 0.9$ fm. $V_{NN}^M(2r_M+2r_N)$ is the pointlike contribution of meson $M$ to the $np$ potential in the $^3S_1$ channel at $r=2r_M+2r_N$ assuming quark-model relations for the coupling constants and using $(g_{NN\pi})^2/4\pi \simeq 15$ and $(g_{NN\rho})^2/4\pi \simeq 0.6$.

| Meson | Mass (MeV) | $\exp[-m(2r_N+2r_M)]$ | $V_{NN}^M(2r_N+2r_M)$ (MeV) |
|---|---|---|---|
| $\pi$ | 140 | $2.6\times10^{-1}$ | $-2.2$ |
| $\eta$ | 548 | $5.1\times10^{-3}$ | $+0.04$ |
| $\eta'$ | 958 | $9.7\times10^{-5}$ | $\sim 0$ |
| $\rho$ | 770 | $1.8\times10^{-4}$ | $-0.02$ |
| $\omega$ | 783 | $1.6\times10^{-4}$ | $+0.06$ |
| $P$-wave $q\bar{q}$ [a] | $\sim 1200$ | $2.4\times10^{-7}$ | $\sim 0$ |
| $D$-wave $q\bar{q}$ | $\sim 1700$ | $5.7\times10^{-12}$ | $\sim 0$ |

[a]These states include the lowest-lying scalar mesons.

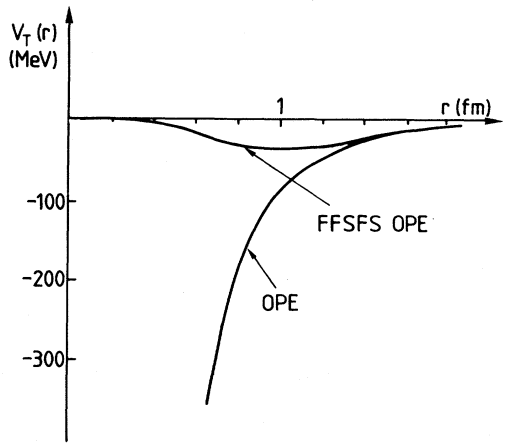


FIG. 4. The FFSFS one-pion exchange tensor potential (see Appendix J for details).

Figs. 3 and 4). The procedure of adding quark and modified meson contributions to obtain the full potential is not rigorously justifiable. Nonetheless, the two regimes seem well enough segregated that one can reasonably hope to obtain a good qualitative understanding of the system at all scales within such a framework. Bearing these limitations in mind, however, we have made no attempt to "fine tune" the pion potential: we have only insisted that the suppression be operative below roughly 2 fm. With hybrid potentials having this character we always obtain a good qualitative description of the deuteron. Our results are given in Table III. Figure 5 shows our deuteron wave functions. The theoretical errors we quote in Table III are rough estimates and arise mainly from two sources: our difficulties with the spurious van der Waals tail of Fig. 1 and uncertainties associated with the semiquantitative implementation of the suppression of the short-distance parts of meson exchange. While we do know that the van der Waals tail should be cut off somewhere in the region $r \gtrsim 2.5$ fm, where pair creation will begin to set in and our empirical knowledge of the interquark potential is weak, it is difficult to prescribe exactly where and how this cutoff should be implemented. However, if we arbitrarily truncate the residual nucleon-nucleon potential in the neighborhood of 2.5 fm, then the $^1S_0$ state indeed unbinds. In fact (after taking into account that the $J=1$ and $J=0$ ground states sample the spurious van der Waals tail differently) the difference in energy between the two channels can be estimated more accurately than the energy of either channel separately. Our result is $E_d - E(^1S_0) = 2.3 \pm 0.3$ MeV.

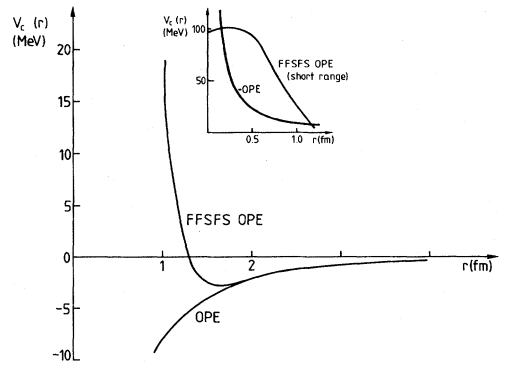


FIG. 3. Central components of the FFSFS one-pion exchange (OPE) potential (see Appendix J for details) and pointlike OPE (the negative of which is shown in the inset).

## V. DISCUSSION

While there are reasons to be cautious (some which we have already mentioned and others which we will discuss below) one might optimistically interpret our results as evidence that even the present rather crude models for QCD are capable of explaining many of the basic features of low-energy nuclear physics. Among those features are the very existence of nucleons in the nucleus, the repulsive core, and the intermediate range attractive nuclear force. We have also, though on less firm grounds, proposed a hybrid model for combining the interactions arising from interquark forces and meson exchange, a model which provides a reasonable quantitative understanding of the simplest nontrivial nucleus, the deuteron.

We believe that, in spite of obvious reservations and bearing in mind the imprecision of certain features of the

TABLE III. Some properties of the six-quark ground states.

| Property | Theoretical value | Experimental value |
|---|---|---|
| $E_d$ (MeV) | $-2.9\ ^{+0.8}_{-0.3}$ | $-2.23$ |
| $(r_d^2)^{1/2}$ (fm) | $2.2 \pm 0.5$ | 1.95 |
| $Q_d$ (mb) | $+2.1 \pm 0.5$ | $+2.86$ |
| $\mu_d$ [a] | $+0.859 \pm 0.003\ \mu_N$ | $+0.857\ \mu_N$ |
| $E(^1S_0)$ (MeV) | $-0.4\ ^{+0.4}_{-0.1}$ | Unbound |

[a]$\mu_d$ is calculated assuming that the departure from $\mu_p+\mu_n$ is due only to our 3.6% $D$-wave mixing.

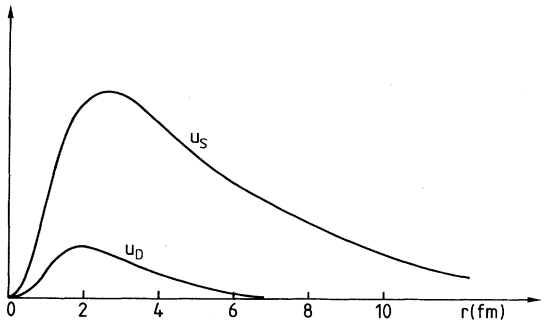


FIG. 5. The deuteron wave functions $u_S$ and $u_D$ of Appendix J, shown with their correct relative normalization.

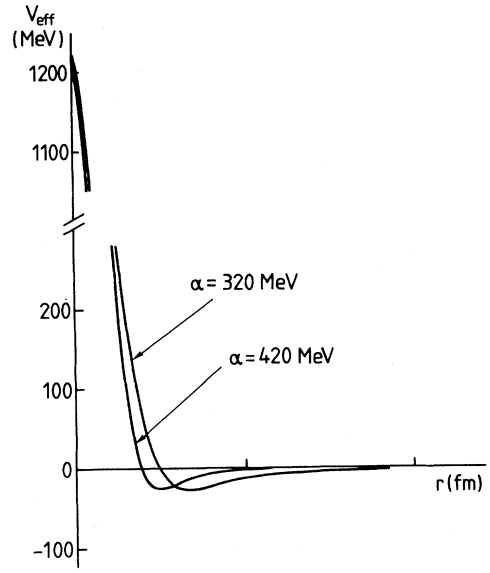


FIG. 6. The dependence of the effective potential on the inverse cluster size $\alpha$ in the $J=1$ channel.

results, it is reasonable to adopt this optimistic interpretation. We have already discussed some of the errors associated with the spurious van der Waals tail and with our semiquantitative suppression of short-distance mesonic effects. We should also mention that, while the existence of the repulsive cores in Fig. 1 is unambiguously demonstrated by the strong suppression of the wave function $\psi(r)$ as $r\to 0$, the magnitude of the repulsion at $r=0$ is less sensitively determined than is the attractive region and could, we estimate, be in error by as much as 20%. Such an error typifies the sort of accuracy we expect from wave-function-sensitive quantities in a variational calculation within such a limited variational space.

Many of our reservations could be dispelled by improvements in the calculation, but unfortunately all those of which we are aware require a considerable increase in effort. It would be especially interesting to perform a fuller variational calculation in which cluster sizes were no longer fixed beforehand but variationally determined and in which intercluster wave functions were allowed to vary independently for distinct cluster configurations. This would, among other things, allow us to complete the proof of our conclusion that three-quark clustering completely dominates the deuteron, since the results of this more complete calculation would be completely independent of the initial cluster decomposition chosen. [The present calculation can, as we have indicated, only draw firm conclusions on other clusterings (like $q^6$) when the system as a whole has a size comparable to the fixed cluster size. The absence of large-scale non-$q^3q^3$ clusterings must be inferred at present from the absence of any substantial configuration mixing to any states whatsoever in the adiabatic approximation, for $r$ much greater than the cluster size.] However, such a calculation, apart from requiring the evaluation of more complicated matrix elements and a restudy of baryon spectroscopy using more realistic spatial dependences for the spin-spin and $U$ potentials, would require a considerable increase in computer time. For the moment we can only offer Fig. 6 as an indication that our results might be stable under such variations. It would also be useful to redo the calculation using a more realistic potential in place of the $U$-perturbed harmonic potential; although our main conclusions should be model independent, the precise form of $V_{\rm eff}$ will not be. In addition one should consider, in more detail than we have done so far, several other issues, among them the effects of such inter-quark spin-orbit potentials as are allowed by baryons, and corrections to (8) from the weak-binding approximation[27] and from possible forbidden states.[28]

There are two possible extensions of this work which we would find especially interesting. Given the dynamical nature of the repulsive core, it seems very likely (if not apparent) that the effective potential in the region out to about 2 fm will depend on the quantum numbers of the $NN$ channel being studied. We see no reason why a calculation in, for example, the $^3P_J$ and $^1P_1$ channels might not reveal the origins of the spin-orbit and non-OPE component of the tensor internucleon interactions, just as the present calculation revealed the non-OPE component of the spin-spin interaction. It would also be interesting to extend our calculation in the $3u$-$3d$ sector to channels with non-$NN$ quantum numbers and also to consider states containing strange quarks in search of possible relatively deeply bound strange analogs of the deuteron.

Finally, we believe it would be very useful to perform calculations using the resonating-group method (or one of its relatives) based on our approach. In particular, our results strongly suggest that the inclusion of $P$-wave color-octet states in such a calculation will produce output phase shifts more like those observed experimentally than has previously been the case. If so, it would certainly further increase our confidence that at least the rudiments of nuclear physics can be understood on the basis of the quark model and that it will eventually be possible to rigorously understand the origins of this subject in QCD.

## ACKNOWLEDGMENTS

We are grateful to the Natural Sciences and Engineering Research Council of Canada for supporting this

research, to G. Luste and A. Pezacki for bearing with us during some periods where we required more computing than we had expected, to the Department of Theoretical Physics and St. John's College of the University of Oxford (where this report was composed and typed) for their hospitality, and to M. Harvey, C. H. Llewellyn Smith, and P. Collins for comments on the work. Finally, K.M. would like to acknowledge the importance of P.B. in the final phases of the calculation and N.I. the value to him of a long series of discussions relevant to this work with O. W. Greenberg and H. J. Lipkin.

## APPENDIX A: CONVENTIONS FOR THE PERMUTATION GROUP $S_3$

There are three irreducible representations $S$, $A$, and $M\equiv(\rho,\lambda)$ labeled by their permutational symmetry (symmetric, antisymmetric, and mixed symmetry, respectively), of dimensions 1, 1, and 2. We adhere to the following convention for the transformation of the basis states of the mixed representation under the transpositions $\pi_{ij}$, those for $S$, $A$ being obvious:

$$\begin{aligned}&\pi_{12}\rho=-\rho, \qquad \pi_{12}\lambda=\lambda\ ,\\ &\pi_{13}\rho=\tfrac{1}{2}\rho-\frac{\sqrt{3}}{2}\lambda, \quad \pi_{13}\lambda=-\frac{\sqrt{3}}{2}\rho-\tfrac{1}{2}\lambda\ ,\\ &\pi_{23}\rho=\tfrac{1}{2}\rho+\frac{\sqrt{3}}{2}\lambda, \quad \pi_{23}\lambda=+\frac{\sqrt{3}}{2}\rho-\tfrac{1}{2}\lambda\ .\end{aligned} \tag{A1}$$

These transformation properties are useful for deriving relations among matrix elements of two-body operators between states of fixed $S_3^u\times S_3^d$ symmetry. The Clebsch-Gordan decompositions of the products of irreducible representations are as follows (here $R$ is any irreducible representation, $\tilde{M}=M$, $\tilde{S}=A$, and $\tilde{A}=S$):

$$\begin{aligned}&S\otimes R=R\ ,\\ &A\otimes R=\tilde{R}\ ,\\ &M\otimes M=S\oplus M\oplus A\ .\end{aligned} \tag{A2}$$

With the above convention for states belonging to $M$ the irreducible components of $M\otimes M$ are as follows:

$$\begin{aligned}&S_{M\otimes M}=\frac{1}{\sqrt{2}}(\rho\rho+\lambda\lambda)\ ,\\ &A_{M\otimes M}=\frac{1}{\sqrt{2}}(\rho\lambda-\lambda\rho)\ ,\\ &\rho_{M\otimes M}=\frac{1}{\sqrt{2}}(\rho\lambda+\lambda\rho)\ ,\\ &\lambda_{M\otimes M}=\frac{1}{\sqrt{2}}(\rho\rho-\lambda\lambda)\ .\end{aligned} \tag{A3}$$

The irreducible representations $S$ and $A$ are one dimensional so that Clebsch-Gordan coefficients for products involving either one of them are trivially unity.

## APPENDIX B: PHASE-I BASIS STATES

The phase-I basis consists of all states separately antisymmetrized in three $u$ and three $d$ quarks having net color zero, net spin 0 or 1, and spatial wave functions constructed from ground-state three-quark clusters in a relative $S$ wave. In order to obtain such states using the Clebsch-Gordan decompositions of Appendix A it is necessary to form bases in each sector having well-defined $S_3^u\times S_3^d$ transformation properties.

In the color sector, recalling that for $SU(3)_c$

$$3\otimes 3\otimes 3=10^S\oplus 8^\rho\oplus 8^\lambda\oplus 1^A \tag{B1}$$

and that none of $10\otimes 10$, $10\otimes 8$, $10\otimes 1$, $8\otimes 1$ contain 1, we see that the possible color-singlet combinations of three $u$ and three $d$ quarks are

$$A^u\circ A^d,\ \ M^u\circ M'^d\ (M,M'=\rho,\lambda)\ , \tag{B2}$$

where

$$A^u\circ A^d\equiv|A^u\rangle\,|A^d\rangle\ , \tag{B3}$$

$$M^u\circ M'^d\equiv\frac{1}{\sqrt{8}}\sum_k|M_k^u\rangle\,|M_k'^d\rangle\ , \tag{B4}$$

and we have simplified the notation by writing $M$ for $8^M$ and $A$ for $1^A$. The two octets $\rho$ and $\lambda$ transform as members of a mixed $S_3$ permutational representation and in accord with the conventions of Appendix A. In normalized form the three-quark color states $\rho_k$, $\lambda_k$ $(k=1,\ldots,8)$, and $A$ are given by

$$|\rho_k\rangle=\tfrac{1}{2}\lambda^k_{\delta\gamma}\epsilon^{\alpha\beta\delta}\,|q^\alpha q^\beta q^\gamma\rangle\ , \tag{B5}$$

$$|\lambda_k\rangle=\frac{1}{\sqrt{3}}(\tfrac{1}{2}\lambda^k_{\delta\gamma}\epsilon^{\alpha\beta\delta}\,|q^\alpha q^\beta q^\gamma\rangle-\lambda^k_{\delta\gamma}\epsilon^{\alpha\beta\delta}\,|q^\gamma q^\beta q^\alpha\rangle)\ , \tag{B6}$$

$$|A\rangle=\frac{1}{\sqrt{6}}\epsilon^{\alpha\beta\gamma}\,|q^\alpha q^\beta q^\gamma\rangle\ , \tag{B7}$$

where $\lambda^k_{\delta\gamma}$ are the elements of the usual Gell-Mann matrices. Similarly, for $SU(2)_{\text{spin}}$

$$\tfrac{1}{2}\otimes\tfrac{1}{2}\otimes\tfrac{1}{2}=\tfrac{3}{2}^S\oplus\tfrac{1}{2}^\rho\oplus\tfrac{1}{2}^\lambda\ . \tag{B8}$$

The following choices are in conformity with the conventions of Appendix A, where we display explicitly only that component of the spin multiplet with maximum projection

$$|\rho\uparrow\rangle=\frac{1}{\sqrt{2}}(\uparrow\downarrow\uparrow-\downarrow\uparrow\uparrow)\ , \tag{B9}$$

$$|\lambda\uparrow\rangle=\frac{-1}{\sqrt{6}}(\uparrow\downarrow\uparrow+\downarrow\uparrow\uparrow-2\uparrow\uparrow\downarrow)\ , \tag{B10}$$

$$|S^{\frac{3}{2}}\rangle=\uparrow\uparrow\uparrow\ . \tag{B11}$$

States of three $u$ and three $d$ quarks with either spin 0 or 1 are then easily constructed using the standard SU(2) Clebsch-Gordan coefficients. The available $S_3^u\times S_3^d$ symmetries are $(SS)$ or $(MM')$ for the $S=0$ channel and $(SS)$, $(MM')$, $(SM)$, and $(MS)$ in the $S=1$ channel, where $M,M'=\rho,\lambda$.

Finally, in the spatial sector, let us introduce the compressed notation $(126;453)\equiv\phi(126)\phi(453)\Psi(\vec{\mathrm{R}}_{126;453})$, etc., where $\phi$ is the ground-state baryon cluster wave function,[2]

TABLE IV. Normalized spatial wave functions with specific $S_3^u \times S_3^d$ symmetry. All states are denoted by their type and $S_3^u \times S_3^d$ symmetry, the $u$ symmetry being listed first.

$$(SS)_{\rm I}=(123;456)$$
$$(SS)_{\rm II}=[(125;463)+(135;462)+(235;461)+(126;453)+(136;452)+(236;451)+(124;563)+(134;562)+(234;561)]/3[(1+8B)]^{1/2}$$
$$(S\rho)_{\rm II}=[(125;463)+(135;462)+(235;461)-(124;563)-(134;562)-(234;561)]/[6(1-B)]^{1/2}$$
$$(S\lambda)_{\rm II}=-[(125;463)+(135;462)+(235;461)+(124;563)+(134;562)+(234;561)-2(126;453)-2(136;452)-2(236;451)]/3[2(1-B)]^{1/2}$$
$$(\rho S)_{\rm II}=[(135;462)+(134;562)+(136;452)-(235;461)-(234;561)-(236;451)]/[6(1-B)]^{1/2}$$
$$(\lambda S)_{\rm II}=-[(235;461)+(135;462)+(234;561)+(134;562)+(236;451)+(136;452)-2(125;463)-2(124;563)-2(126;453)]/3[2(1-B)]^{1/2}$$
$$(\rho\rho)_{\rm II}=[(135;462)-(235;461)-(134;562)+(234;561)]/2[(1-B)]^{1/2}$$
$$(\rho\lambda)_{\rm II}=-[(135;462)-(235;461)+(134;562)-(234;561)-2(136;452)+2(236;451)]/2[3(1-B)]^{1/2}$$
$$(\lambda\rho)_{\rm II}=-[(235;461)+(135;462)-2(125;463)-(234;561)-(134;562)+2(124;563)]/2[3(1-B)]^{1/2}$$
$$(\lambda\lambda)_{\rm II}=[(235;461)+(135;462)-2(125;463)+(234;561)+(134;562)-2(124;563)-2(236;451)-2(136;452)+4(126;453)]/6(1-B)^{1/2}$$

$$\phi(126)=\frac{\alpha^3}{\pi^{3/2}}\exp[-\tfrac{1}{2}\alpha^2(\rho_{126}{}^2+\lambda_{126}{}^2)]\ , \tag{B12}$$

$\Psi$ is the intercluster wave function depending only on the separation of the centers of mass of the two clusters,

$$\vec{\mathbf{R}}_{126;453}=\tfrac{1}{3}(\vec{\mathbf{r}}_1+\vec{\mathbf{r}}_2+\vec{\mathbf{r}}_6)-\tfrac{1}{3}(\vec{\mathbf{r}}_4+\vec{\mathbf{r}}_5+\vec{\mathbf{r}}_3) \tag{B13}$$

and $\vec{\rho}_{126}, \vec{\lambda}_{126}$ are the usual Jacobi coordinates for the cluster 126,

$$\vec{\rho}_{126}=\frac{1}{\sqrt{2}}(\vec{\mathbf{r}}_1-\vec{\mathbf{r}}_2)\ , \tag{B14}$$

$$\vec{\lambda}_{126}=\frac{1}{\sqrt{6}}(\vec{\mathbf{r}}_1+\vec{\mathbf{r}}_2-2\vec{\mathbf{r}}_6)\ , \tag{B15}$$

which transform as suggested by the notation under $S_3^{126}$. The wave function (126;453) is assumed normalized in the center-of-mass system with respect to the measure $d\tau_{126;453}\equiv d^3R_{126;453}d^3\rho_{126}d^3\rho_{453}d^3\lambda_{126}d^3\lambda_{453}$. If we represent $\Psi$ by a sum of Gaussians

$$\Psi(\vec{\mathbf{r}})=N\sum_{i=1}^{i_{\max}}\xi_i\exp(-\tfrac{1}{2}\beta_i{}^2r^2) \tag{B16}$$

then the normalization constant $N$ is given by

$$N=\frac{1}{\pi^{3/4}}\left[\sum_{i,j}\xi_i\xi_j(\tfrac{1}{2}\beta_i{}^2+\tfrac{1}{2}\beta_j{}^2)^{-3/2}\right]^{-1/2}\equiv\frac{F^{-1/2}}{\pi^{3/4}}\ . \tag{B17}$$

The use of such nonlinear parametrizations is well established in cluster calculations in nuclear physics.[24] We will henceforth label the $u$ quarks 1,2,3 and the $d$ quarks 4,5,6. From the ten distinct spatial states $(ijk;lmn)$ $(ijk;lmn$ any partition of $\{1,\ldots,6\})$ one may easily construct normalized spatial states having definite $S_3^u\times S_3^d$ transformation properties. These states are listed in Table IV. Note that there are two states with spatial symmetry $(SS)$, of types I and II, consisting of $uuu,ddd$ and $uud,ddu$ clusters, respectively. These states are not, in general, orthogonal, but orthogonal combinations are easily constructed. The quantity $B$ in Table IV is the exchange overlap integral

$$B=\int d\tau_{126;453}(126;453)^*(125;463)\ . \tag{B18}$$

There is only one such integral owing to the spatial symmetry of the clusters and the invariance of $\Psi$ under cluster interchange.

The phase-I basis states are now straightforward to construct. We list below these states for the spin-0 and -1 channels. The notation is such that, reading left to right, one encounters symmetry labels in the order space($u$), space($d$), spin($u$), spin($d$), color($u$), color($d$). The spins are coupled to the appropriate total spin. The subscripts I (II) refer to the type of clustering in the event the spatial symmetry is $(SS)$. In the $S=0$ channel we have

$$|1\rangle=(SSSSAA)_{\rm II}\ , \tag{B19}$$

$$|2\rangle=\tfrac{1}{2}[(\rho\rho\rho\rho AA)+(\rho\lambda\rho\lambda AA)+(\lambda\rho\lambda\rho AA)+(\lambda\lambda\lambda\lambda AA)]\ , \tag{B20}$$

$$|3\rangle=\tfrac{1}{2}[(SS\lambda\lambda\rho\rho)_{\rm II}+(SS\rho\rho\lambda\lambda)_{\rm II}-(SS\rho\lambda\lambda\rho)_{\rm II}-(SS\lambda\rho\rho\lambda)_{\rm II}]\ , \tag{B21}$$

$$|4\rangle=\tfrac{1}{2}[(\lambda\lambda SS\rho\rho)+(\rho\rho SS\lambda\lambda)-(\rho\lambda SS\lambda\rho)-(\lambda\rho SS\rho\lambda)]\ , \tag{B22}$$

$$|5\rangle=\frac{-1}{2\sqrt{2}}[(S\rho\lambda\rho\rho\rho)-(S\lambda\lambda\lambda\rho\rho)+(S\rho\rho\lambda\lambda\lambda)+(S\lambda\rho\rho\lambda\lambda)-(S\rho\rho\rho\lambda\rho)+(S\lambda\rho\lambda\lambda\rho)-(S\rho\lambda\lambda\rho\lambda)-(S\lambda\lambda\rho\rho\lambda)]\ , \tag{B23}$$

$$|6\rangle=\frac{-1}{2\sqrt{2}}[(\rho S\rho\lambda\rho\rho)-(\lambda S\lambda\lambda\rho\rho)+(\lambda S\rho\rho\lambda\lambda)+(\rho S\lambda\rho\lambda\lambda)-(\lambda S\rho\lambda\lambda\rho)-(\rho S\lambda\lambda\lambda\rho)-(\rho S\rho\rho\rho\lambda)+(\lambda S\lambda\rho\rho\lambda)]\ , \tag{B24}$$

$$|7\rangle=\tfrac{1}{4}[(\rho\rho\rho\rho\rho\rho)-(\rho\lambda\rho\lambda\rho\rho)-(\lambda\rho\lambda\rho\rho\rho)+(\lambda\lambda\lambda\lambda\rho\rho)+(\rho\rho\lambda\lambda\lambda\lambda)+(\rho\lambda\lambda\rho\lambda\lambda)$$
$$+(\lambda\rho\rho\lambda\lambda\lambda)+(\lambda\lambda\rho\rho\lambda\lambda)-(\rho\rho\lambda\rho\lambda\rho)-(\lambda\rho\rho\rho\lambda\rho)+(\rho\lambda\lambda\lambda\lambda\rho)$$
$$+(\lambda\lambda\rho\lambda\lambda\rho)-(\rho\rho\rho\lambda\rho\lambda)-(\rho\lambda\rho\rho\rho\lambda)+(\lambda\rho\lambda\lambda\rho\lambda)+(\lambda\lambda\lambda\rho\rho\lambda)]\ , \tag{B25}$$

$$|8\rangle=(\mathrm{II}\rightarrow\mathrm{I})\,|1\rangle\ , \tag{B26}$$

$$|9\rangle=(\mathrm{II}\rightarrow\mathrm{I})\,|3\rangle\ . \tag{B27}$$

All states from the $S=0$ sector can be recoupled to $S=1$. States $|1\rangle$ through $|7\rangle$ in the $S=1$ sector are therefore labeled as in $|1\rangle$ through $|7\rangle$ of the $S=0$ sector. The states $|8\rangle$ and $|9\rangle$ of that sector, under recoupling, become states $|14\rangle$ and $|15\rangle$, respectively, of $S=1$. The remaining states are

$$|8\rangle=\tfrac{1}{2}[(S\lambda\lambda S\rho\rho)+(S\rho\rho S\lambda\lambda)-(S\lambda\rho S\lambda\rho)-(S\rho\lambda S\rho\lambda)]\ , \tag{B28}$$

$$|9\rangle=\tfrac{1}{2}[(\lambda SS\lambda\rho\rho)+(\rho SS\rho\lambda\lambda)-(\lambda SS\rho\rho\lambda)-(\rho SS\lambda\lambda\rho)]\ , \tag{B29}$$

$$|10\rangle=\frac{-1}{2\sqrt{2}}[(\rho\lambda\rho S\rho\rho)-(\lambda\lambda\lambda S\rho\rho)+(\rho\rho\lambda S\lambda\lambda)+(\lambda\rho\rho S\lambda\lambda)-(\rho\lambda\lambda S\lambda\rho)-(\lambda\lambda\rho S\lambda\rho)-(\rho\rho\rho S\rho\lambda)+(\lambda\rho\lambda S\rho\lambda)]\ , \tag{B30}$$

$$|11\rangle=\frac{-1}{2\sqrt{2}}[(\lambda\rho S\rho\rho\rho)-(\lambda\lambda S\lambda\rho\rho)+(\rho\rho S\lambda\lambda\lambda)+(\rho\lambda S\rho\lambda\lambda)-(\rho\rho S\rho\lambda\rho)+(\rho\lambda S\lambda\lambda\rho)-(\lambda\rho S\lambda\rho\lambda)-(\lambda\lambda S\rho\rho\lambda)]\ , \tag{B31}$$

$$|12\rangle=\frac{1}{\sqrt{2}}[(S\rho S\rho AA)+(S\lambda S\lambda AA)]\ , \tag{B32}$$

$$|13\rangle=\frac{1}{\sqrt{2}}[(\rho S\rho SAA)+(\lambda S\lambda SAA)]\ . \tag{B33}$$

The matrix elements of the various components of the Hamiltonian $H$ can be constructed in this basis from the color, spin, and spatial matrix elements listed in Appendices C, D, and E, respectively. In fact, owing to the antisymmetry of the states we have for any symmetric operator $V_{ij}$

$$\langle A\,|\sum_{i<j}V_{ij}\,|\,B\rangle=\langle A\,|\,3V_{12}+3V_{45}+9V_{14}\,|\,B\rangle \tag{B34}$$

for all states $|A\rangle$ and $|B\rangle$. In the tables of these appendices we list enough matrix elements to enable the reader to check their consistency.

## APPENDIX C: COLOR MATRIX ELEMENTS

We note that the color dependence of the quark Hamiltonian is contained entirely in the factor $\Lambda_{ij}^{c}\equiv\sum_k(\frac{1}{2}\lambda^k)_i(\frac{1}{2}\lambda^k)_j$, $i$ and $j$ being particle labels. The matrix elements of $\Lambda_{ij}^{c}$ relative to the color-singlet basis constructed in Appendix B are given in Table V. As a convenience to the reader we have presented the full table which can, of course, be derived by permutational arguments from a much smaller set of matrix elements.

## APPENDIX D: MATRIX ELEMENTS OF THE SPIN OPERATORS $\vec{S}_i\cdot\vec{S}_j$

The spin states of the $S=0$ and 1 channels have been discussed in Appendix B. Using the spherical decomposition

$$\vec{S}_i\cdot\vec{S}_j=\tfrac{1}{2}(S_{i+}S_{j-}+S_{i-}S_{j+})+S_{iz}S_{jz}\ , \tag{D1}$$

where $S_{\pm}$ are the usual spin-raising and lowering operators ($S_{\pm}=S_x\pm iS_y$ so that $\mp S_{\pm}/\sqrt{2}$ are the usual spherical components of $\vec{S}$), one may readily generate the results of Tables VI and VII. Note that the relative sign of our spin states $(MS)_{S=1}$ and $(SM)_{S=1}$ differs from the standard Condon-Shortley convention since we relate these two states by simply interchanging $u$'s with $d$'s. Care must therefore be exercised in deriving spin-1 matrix elements using permutational techniques. As in Appendix C we list all matrix elements for the reader's convenience.

## APPENDIX E: PHASE-I SPATIAL MATRIX ELEMENTS

Given the basis of normalized spatial states with definite $S_3^u\times S_3^d$ symmetries constructed in Appendix B one can readily generate all matrix elements for a particular symmetric two-body operator $\Lambda_{ij}$. $\Lambda_{ij}$ is given by $(\vec{r}_i-\vec{r}_j)^2\equiv\vec{r}_{ij}^{\,2}$ for the confinement potential and $\delta^3(\vec{r}_{ij})$ for both the $U$ and hyperfine potentials. Permutational symmetries allow all matrix elements to be generated from a smaller set involving only a limited number of $S_3^u\times S_3^d$ symmetries and these in turn can be expressed in terms of the following quantities.

(1) Direct matrix elements. Since a given pair $ij$ either both lie in the same cluster or lie in different clusters there are two matrix elements of this type:

$$\begin{bmatrix}s\\n\end{bmatrix}\equiv\int d\tau_{126;435}(126;435)^*\begin{bmatrix}\Lambda_{12}\\\Lambda_{14}\end{bmatrix}(126;435)\ . \tag{E1}$$

(2) Exchange matrix elements. From the permutational symmetry of the three-quark subclusters one sees that there are four distinct matrix elements of this type:

TABLE V. The color matrix elements $\langle l'_u l'_d \mid \Lambda^c_{ij} \mid l_u l_d \rangle$. $l_u$ ($l_d$) are the symmetry labels of the states with respect to the group $S_3^u$ ($S_3^d$).

| $l'_u l'_d$ | $l_u l_d$ | 12 | 13 | 23 | 45 | 46 | 56 | 14 | 15 | 16 | 24 | 25 | 26 | 34 | 35 | 36 |
|---|---|---|---|---|---|---|---|---|---|---|---|---|---|---|---|---|
| $AA$ | $AA$ | $-\frac{2}{3}$ | $-\frac{2}{3}$ | $-\frac{2}{3}$ | $-\frac{2}{3}$ | $-\frac{2}{3}$ | $-\frac{2}{3}$ | 0 | 0 | 0 | 0 | 0 | 0 | 0 | 0 | 0 |
| $AA$ | $\rho\rho$ | 0 | 0 | 0 | 0 | 0 | 0 | $1/6\sqrt{2}$ | $1/6\sqrt{2}$ | $-1/3\sqrt{2}$ | $1/6\sqrt{2}$ | $1/6\sqrt{2}$ | $-1/3\sqrt{2}$ | $-1/3\sqrt{2}$ | $-1/3\sqrt{2}$ | $2/3\sqrt{2}$ |
| $AA$ | $\rho\lambda$ | 0 | 0 | 0 | 0 | 0 | 0 | $-1/2\sqrt{6}$ | $1/2\sqrt{6}$ | 0 | $-1/2\sqrt{6}$ | $1/2\sqrt{6}$ | 0 | $1/\sqrt{6}$ | $-1/\sqrt{6}$ | 0 |
| $AA$ | $\lambda\rho$ | 0 | 0 | 0 | 0 | 0 | 0 | $-1/2\sqrt{6}$ | $-1/2\sqrt{6}$ | $1/\sqrt{6}$ | $1/2\sqrt{6}$ | $1/2\sqrt{6}$ | $-1/\sqrt{6}$ | 0 | 0 | 0 |
| $AA$ | $\lambda\lambda$ | 0 | 0 | 0 | 0 | 0 | 0 | $1/2\sqrt{2}$ | $-1/2\sqrt{2}$ | 0 | $-1/2\sqrt{2}$ | $1/2\sqrt{2}$ | 0 | 0 | 0 | 0 |
| $\rho\rho$ | $\rho\rho$ | $-\frac{2}{3}$ | $\frac{1}{12}$ | $\frac{1}{12}$ | $-\frac{2}{3}$ | $\frac{1}{12}$ | $\frac{1}{12}$ | $-\frac{1}{12}$ | $-\frac{1}{12}$ | $-\frac{7}{12}$ | $-\frac{1}{12}$ | $-\frac{1}{12}$ | $-\frac{7}{12}$ | $-\frac{7}{12}$ | $-\frac{7}{12}$ | $-\frac{1}{3}$ |
| $\rho\rho$ | $\rho\lambda$ | 0 | 0 | 0 | 0 | $-3/4\sqrt{3}$ | $3/4\sqrt{3}$ | $1/2\sqrt{3}$ | $-1/2\sqrt{3}$ | 0 | $1/2\sqrt{3}$ | $-1/2\sqrt{3}$ | 0 | $-1/4\sqrt{3}$ | $1/4\sqrt{3}$ | 0 |
| $\rho\rho$ | $\lambda\rho$ | 0 | $-3/4\sqrt{3}$ | $3/4\sqrt{3}$ | 0 | 0 | 0 | $1/2\sqrt{3}$ | $1/2\sqrt{3}$ | $-1/4\sqrt{3}$ | $-1/2\sqrt{3}$ | $-1/2\sqrt{3}$ | $1/4\sqrt{3}$ | 0 | 0 | 0 |
| $\rho\rho$ | $\lambda\lambda$ | 0 | 0 | 0 | 0 | 0 | 0 | $\frac{1}{4}$ | $-\frac{1}{4}$ | 0 | $-\frac{1}{4}$ | $\frac{1}{4}$ | 0 | 0 | 0 | 0 |
| $\rho\lambda$ | $\rho\lambda$ | $-\frac{2}{3}$ | $\frac{1}{12}$ | $\frac{1}{12}$ | $\frac{1}{3}$ | $-\frac{5}{12}$ | $-\frac{5}{12}$ | $-\frac{5}{12}$ | $-\frac{5}{12}$ | $\frac{1}{12}$ | $-\frac{5}{12}$ | $-\frac{5}{12}$ | $\frac{1}{12}$ | $-\frac{5}{12}$ | $-\frac{5}{12}$ | $-\frac{2}{3}$ |
| $\rho\lambda$ | $\lambda\rho$ | 0 | 0 | 0 | 0 | 0 | 0 | $\frac{1}{4}$ | $-\frac{1}{4}$ | 0 | $-\frac{1}{4}$ | $\frac{1}{4}$ | 0 | 0 | 0 | 0 |
| $\rho\lambda$ | $\lambda\lambda$ | 0 | $-3/4\sqrt{3}$ | $3/4\sqrt{3}$ | 0 | 0 | 0 | 0 | 0 | $3/4\sqrt{3}$ | 0 | 0 | $-3/4\sqrt{3}$ | 0 | 0 | 0 |
| $\lambda\rho$ | $\lambda\rho$ | $\frac{1}{3}$ | $-\frac{5}{12}$ | $-\frac{5}{12}$ | $-\frac{2}{3}$ | $\frac{1}{12}$ | $\frac{1}{12}$ | $-\frac{5}{12}$ | $-\frac{5}{12}$ | $-\frac{5}{12}$ | $-\frac{5}{12}$ | $-\frac{5}{12}$ | $-\frac{5}{12}$ | $\frac{1}{12}$ | $\frac{1}{12}$ | $-\frac{2}{3}$ |
| $\lambda\rho$ | $\lambda\lambda$ | 0 | 0 | 0 | 0 | $-3/4\sqrt{3}$ | $3/4\sqrt{3}$ | 0 | 0 | 0 | 0 | 0 | 0 | $3/4\sqrt{3}$ | $-3/4\sqrt{3}$ | 0 |
| $\lambda\lambda$ | $\lambda\lambda$ | $\frac{1}{3}$ | $-\frac{5}{12}$ | $-\frac{5}{12}$ | $\frac{1}{3}$ | $-\frac{5}{12}$ | $-\frac{5}{12}$ | $-\frac{5}{12}$ | $-\frac{5}{12}$ | $-\frac{5}{12}$ | $-\frac{5}{12}$ | $-\frac{5}{12}$ | $-\frac{5}{12}$ | $-\frac{5}{12}$ | $-\frac{5}{12}$ | $\frac{1}{3}$ |

TABLE VI. Spin-zero matrix elements $\langle l'_u l'_d \mid \vec{S}_i \cdot \vec{S}_j \mid l_u l_d \rangle$. Notation and format as in Table V.

| $l'_u l'_d$ | $l_u l_d$ | 12 | 13 | 23 | 45 | 46 | 56 | 14 | 15 | 16 | 24 | 25 | 26 | 34 | 35 | 36 |
|---|---|---|---|---|---|---|---|---|---|---|---|---|---|---|---|---|
| $SS$ | $SS$ | $\frac{1}{4}$ | $\frac{1}{4}$ | $\frac{1}{4}$ | $\frac{1}{4}$ | $\frac{1}{4}$ | $\frac{1}{4}$ | $-\frac{5}{12}$ | $-\frac{5}{12}$ | $-\frac{5}{12}$ | $-\frac{5}{12}$ | $-\frac{5}{12}$ | $-\frac{5}{12}$ | $-\frac{5}{12}$ | $-\frac{5}{12}$ | $-\frac{5}{12}$ |
| $SS$ | $\rho\rho$ | 0 | 0 | 0 | 0 | 0 | 0 | $-1/2\sqrt{2}$ | $1/2\sqrt{2}$ | 0 | $1/2\sqrt{2}$ | $-1/2\sqrt{2}$ | 0 | 0 | 0 | 0 |
| $SS$ | $\rho\lambda$ | 0 | 0 | 0 | 0 | 0 | 0 | $-1/2\sqrt{6}$ | $-1/2\sqrt{6}$ | $1/\sqrt{6}$ | $1/2\sqrt{6}$ | $1/2\sqrt{6}$ | $-1/\sqrt{6}$ | 0 | 0 | 0 |
| $SS$ | $\lambda\rho$ | 0 | 0 | 0 | 0 | 0 | 0 | $-1/2\sqrt{6}$ | $1/2\sqrt{6}$ | 0 | $-1/2\sqrt{6}$ | $1/2\sqrt{6}$ | 0 | $1/\sqrt{6}$ | $-1/\sqrt{6}$ | 0 |
| $SS$ | $\lambda\lambda$ | 0 | 0 | 0 | 0 | 0 | 0 | $-1/6\sqrt{2}$ | $-1/6\sqrt{2}$ | $1/3\sqrt{2}$ | $-1/6\sqrt{2}$ | $-1/6\sqrt{2}$ | $1/3\sqrt{2}$ | $1/3\sqrt{2}$ | $1/3\sqrt{2}$ | $-2/3\sqrt{2}$ |
| $\rho\rho$ | $\rho\rho$ | $-\frac{3}{4}$ | 0 | 0 | $-\frac{3}{4}$ | 0 | 0 | 0 | 0 | 0 | 0 | 0 | 0 | 0 | 0 | $-\frac{3}{4}$ |
| $\rho\rho$ | $\rho\lambda$ | 0 | 0 | 0 | 0 | $-3/4\sqrt{3}$ | $3/4\sqrt{3}$ | 0 | 0 | 0 | 0 | 0 | 0 | $3/4\sqrt{3}$ | $-3/4\sqrt{3}$ | 0 |
| $\rho\rho$ | $\lambda\rho$ | 0 | $-3/4\sqrt{3}$ | $3/4\sqrt{3}$ | 0 | 0 | 0 | 0 | 0 | $3/4\sqrt{3}$ | 0 | 0 | $-3/4\sqrt{3}$ | 0 | 0 | 0 |
| $\rho\rho$ | $\lambda\lambda$ | 0 | 0 | 0 | 0 | 0 | 0 | $-\frac{1}{4}$ | $\frac{1}{4}$ | 0 | $\frac{1}{4}$ | $-\frac{1}{4}$ | 0 | 0 | 0 | 0 |
| $\rho\lambda$ | $\rho\lambda$ | $-\frac{3}{4}$ | 0 | 0 | $\frac{1}{4}$ | $-\frac{1}{2}$ | $-\frac{1}{2}$ | 0 | 0 | 0 | 0 | 0 | 0 | $-\frac{1}{2}$ | $-\frac{1}{2}$ | $\frac{1}{4}$ |
| $\rho\lambda$ | $\lambda\rho$ | 0 | 0 | 0 | 0 | 0 | 0 | $-\frac{1}{4}$ | $\frac{1}{4}$ | 0 | $\frac{1}{4}$ | $-\frac{1}{4}$ | 0 | 0 | 0 | 0 |
| $\rho\lambda$ | $\lambda\lambda$ | 0 | $-3/4\sqrt{3}$ | $3/4\sqrt{3}$ | 0 | 0 | 0 | $1/2\sqrt{3}$ | $1/2\sqrt{3}$ | $-1/4\sqrt{3}$ | $-1/2\sqrt{3}$ | $-1/2\sqrt{3}$ | $1/4\sqrt{3}$ | 0 | 0 | 0 |
| $\lambda\rho$ | $\lambda\rho$ | $\frac{1}{4}$ | $-\frac{1}{2}$ | $-\frac{1}{2}$ | $-\frac{3}{4}$ | 0 | 0 | 0 | 0 | $-\frac{1}{2}$ | 0 | 0 | $-\frac{1}{2}$ | 0 | 0 | $\frac{1}{4}$ |
| $\lambda\rho$ | $\lambda\lambda$ | 0 | 0 | 0 | 0 | $-3/4\sqrt{3}$ | $3/4\sqrt{3}$ | $1/2\sqrt{3}$ | $-1/2\sqrt{3}$ | 0 | $1/2\sqrt{3}$ | $-1/2\sqrt{3}$ | 0 | $-1/4\sqrt{3}$ | $1/4\sqrt{3}$ | 0 |
| $\lambda\lambda$ | $\lambda\lambda$ | $\frac{1}{4}$ | $-\frac{1}{2}$ | $-\frac{1}{2}$ | $\frac{1}{4}$ | $-\frac{1}{2}$ | $-\frac{1}{2}$ | $-\frac{1}{3}$ | $-\frac{1}{3}$ | $\frac{1}{6}$ | $-\frac{1}{3}$ | $-\frac{1}{3}$ | $\frac{1}{6}$ | $\frac{1}{6}$ | $\frac{1}{6}$ | $-\frac{1}{12}$ |

TABLE VII. Spin-one matrix elements $\langle l_u' l_d' \mid \vec{S}_i \cdot \vec{S}_j \mid l_u l_d \rangle$. Notation and format as in Table V.

| $l_u' l_d'$ $l_u l_d$ | 12 | 13 | 23 | 45 | 46 | 56 | 14 | 15 | 16 | 24 | 25 | 26 | 34 | 35 | 36 |
|---|---|---|---|---|---|---|---|---|---|---|---|---|---|---|---|
| $SS$ $SS$ | $\frac{1}{4}$ | $\frac{1}{4}$ | $\frac{1}{4}$ | $\frac{1}{4}$ | $\frac{1}{4}$ | $\frac{1}{4}$ | $-\frac{11}{36}$ | $-\frac{11}{36}$ | $-\frac{11}{36}$ | $-\frac{11}{36}$ | $-\frac{11}{36}$ | $-\frac{11}{36}$ | $-\frac{11}{36}$ | $-\frac{11}{36}$ | $-\frac{11}{36}$ |
| $SS$ $S\rho$ | 0 | 0 | 0 | 0 | 0 | 0 | $\sqrt{5}/6\sqrt{3}$ | $-\sqrt{5}/6\sqrt{3}$ | 0 | $\sqrt{5}/6\sqrt{3}$ | $-\sqrt{5}/6\sqrt{3}$ | 0 | $\sqrt{5}/6\sqrt{3}$ | $-\sqrt{5}/6\sqrt{3}$ | 0 |
| $SS$ $S\lambda$ | 0 | 0 | 0 | 0 | 0 | 0 | $\sqrt{5}/18$ | $\sqrt{5}/18$ | $-\sqrt{5}/9$ | $\sqrt{5}/18$ | $\sqrt{5}/18$ | $-\sqrt{5}/9$ | $\sqrt{5}/18$ | $\sqrt{5}/18$ | $-\sqrt{5}/9$ |
| $SS$ $\rho S$ | 0 | 0 | 0 | 0 | 0 | 0 | $\sqrt{5}/6\sqrt{3}$ | $\sqrt{5}/6\sqrt{3}$ | $\sqrt{5}/6\sqrt{3}$ | $-\sqrt{5}/6\sqrt{3}$ | $-\sqrt{5}/6\sqrt{3}$ | $-\sqrt{5}/6\sqrt{3}$ | 0 | 0 | 0 |
| $SS$ $\lambda S$ | 0 | 0 | 0 | 0 | 0 | 0 | $\sqrt{5}/18$ | $\sqrt{5}/18$ | $\sqrt{5}/18$ | $\sqrt{5}/18$ | $\sqrt{5}/18$ | $\sqrt{5}/18$ | $-\sqrt{5}/9$ | $-\sqrt{5}/9$ | $-\sqrt{5}/9$ |
| $SS$ $\rho\rho$ | 0 | 0 | 0 | 0 | 0 | 0 | $-5/6\sqrt{10}$ | $5/6\sqrt{10}$ | 0 | $5/6\sqrt{10}$ | $-5/6\sqrt{10}$ | 0 | 0 | 0 | 0 |
| $SS$ $\rho\lambda$ | 0 | 0 | 0 | 0 | 0 | 0 | $-\sqrt{5}/6\sqrt{6}$ | $-\sqrt{5}/6\sqrt{6}$ | $\sqrt{5}/3\sqrt{6}$ | $\sqrt{5}/6\sqrt{6}$ | $\sqrt{5}/6\sqrt{6}$ | $-\sqrt{5}/3\sqrt{6}$ | 0 | 0 | 0 |
| $SS$ $\lambda\rho$ | 0 | 0 | 0 | 0 | 0 | 0 | $-\sqrt{5}/6\sqrt{6}$ | $\sqrt{5}/6\sqrt{6}$ | 0 | $-\sqrt{5}/6\sqrt{6}$ | $\sqrt{5}/6\sqrt{6}$ | 0 | $\sqrt{5}/3\sqrt{6}$ | $-\sqrt{5}/3\sqrt{6}$ | 0 |
| $SS$ $\lambda\lambda$ | 0 | 0 | 0 | 0 | 0 | 0 | $-\sqrt{5}/18\sqrt{2}$ | $-\sqrt{5}/18\sqrt{2}$ | $\sqrt{5}/9\sqrt{2}$ | $-\sqrt{5}/18\sqrt{2}$ | $-\sqrt{5}/18\sqrt{2}$ | $\sqrt{5}/9\sqrt{2}$ | $\sqrt{5}/9\sqrt{2}$ | $\sqrt{5}/9\sqrt{2}$ | $-2\sqrt{5}/9\sqrt{2}$ |
| $S\rho$ $S\rho$ | $\frac{1}{4}$ | $\frac{1}{4}$ | $\frac{1}{4}$ | $-\frac{3}{4}$ | 0 | 0 | 0 | 0 | $-\frac{5}{12}$ | 0 | 0 | $-\frac{5}{12}$ | 0 | 0 | $-\frac{5}{12}$ |
| $S\rho$ $S\lambda$ | 0 | 0 | 0 | 0 | $-3/4\sqrt{3}$ | $3/4\sqrt{3}$ | $5/12\sqrt{3}$ | $-5/12\sqrt{3}$ | 0 | $5/12\sqrt{3}$ | $-5/12\sqrt{3}$ | 0 | $5/12\sqrt{3}$ | $-5/12\sqrt{3}$ | 0 |
| $S\rho$ $\rho S$ | 0 | 0 | 0 | 0 | 0 | 0 | $-\frac{1}{12}$ | $\frac{1}{12}$ | 0 | $\frac{1}{12}$ | $-\frac{1}{12}$ | 0 | 0 | 0 | 0 |
| $S\rho$ $\lambda S$ | 0 | 0 | 0 | 0 | 0 | 0 | $-1/12\sqrt{3}$ | $1/12\sqrt{3}$ | 0 | $-1/12\sqrt{3}$ | $1/12\sqrt{3}$ | 0 | $1/6\sqrt{3}$ | $-1/6\sqrt{3}$ | 0 |
| $S\rho$ $\rho\rho$ | 0 | 0 | 0 | 0 | 0 | 0 | 0 | 0 | $-1/\sqrt{6}$ | 0 | 0 | $1/\sqrt{6}$ | 0 | 0 | 0 |
| $S\rho$ $\rho\lambda$ | 0 | 0 | 0 | 0 | 0 | 0 | $1/3\sqrt{2}$ | $-1/3\sqrt{2}$ | 0 | $-1/3\sqrt{2}$ | $1/3\sqrt{2}$ | 0 | 0 | 0 | 0 |
| $S\rho$ $\lambda\rho$ | 0 | 0 | 0 | 0 | 0 | 0 | 0 | 0 | $-1/3\sqrt{2}$ | 0 | 0 | $-1/3\sqrt{2}$ | 0 | 0 | $2/3\sqrt{2}$ |
| $S\rho$ $\lambda\lambda$ | 0 | 0 | 0 | 0 | 0 | 0 | $1/3\sqrt{6}$ | $-1/3\sqrt{6}$ | 0 | $1/3\sqrt{6}$ | $-1/3\sqrt{6}$ | 0 | $-2/3\sqrt{6}$ | $2/3\sqrt{6}$ | 0 |
| $S\lambda$ $S\lambda$ | $\frac{1}{4}$ | $\frac{1}{4}$ | $\frac{1}{4}$ | $\frac{1}{4}$ | $-\frac{1}{2}$ | $-\frac{1}{2}$ | $-\frac{5}{18}$ | $-\frac{5}{18}$ | $\frac{5}{36}$ | $-\frac{5}{18}$ | $-\frac{5}{18}$ | $\frac{5}{36}$ | $-\frac{5}{18}$ | $-\frac{5}{18}$ | $\frac{5}{36}$ |
| $S\lambda$ $\rho S$ | 0 | 0 | 0 | 0 | 0 | 0 | $-1/12\sqrt{3}$ | $-1/12\sqrt{3}$ | $1/6\sqrt{3}$ | $1/12\sqrt{3}$ | $1/12\sqrt{3}$ | $-1/6\sqrt{3}$ | 0 | 0 | 0 |
| $S\lambda$ $\lambda S$ | 0 | 0 | 0 | 0 | 0 | 0 | $-\frac{1}{36}$ | $-\frac{1}{36}$ | $\frac{1}{18}$ | $-\frac{1}{36}$ | $-\frac{1}{36}$ | $\frac{1}{18}$ | $\frac{1}{18}$ | $\frac{1}{18}$ | $-\frac{1}{9}$ |
| $S\lambda$ $\rho\rho$ | 0 | 0 | 0 | 0 | 0 | 0 | $1/3\sqrt{2}$ | $-1/3\sqrt{2}$ | 0 | $-1/3\sqrt{2}$ | $1/3\sqrt{2}$ | 0 | 0 | 0 | 0 |
| $S\lambda$ $\rho\lambda$ | 0 | 0 | 0 | 0 | 0 | 0 | $-2/3\sqrt{6}$ | $-2/3\sqrt{6}$ | $1/3\sqrt{6}$ | $2/3\sqrt{6}$ | $2/3\sqrt{6}$ | $-1/3\sqrt{6}$ | 0 | 0 | 0 |
| $S\lambda$ $\lambda\rho$ | 0 | 0 | 0 | 0 | 0 | 0 | $1/3\sqrt{6}$ | $-1/3\sqrt{6}$ | 0 | $1/3\sqrt{6}$ | $-1/3\sqrt{6}$ | 0 | $-2/3\sqrt{6}$ | $2/3\sqrt{6}$ | 0 |
| $S\lambda$ $\lambda\lambda$ | 0 | 0 | 0 | 0 | 0 | 0 | $-2/9\sqrt{2}$ | $-2/9\sqrt{2}$ | $1/9\sqrt{2}$ | $-2/9\sqrt{2}$ | $-2/9\sqrt{2}$ | $1/9\sqrt{2}$ | $4/9\sqrt{2}$ | $4/9\sqrt{2}$ | $-2/9\sqrt{2}$ |
| $\rho S$ $\rho S$ | $-\frac{3}{4}$ | 0 | 0 | $\frac{1}{4}$ | $\frac{1}{4}$ | $\frac{1}{4}$ | 0 | 0 | 0 | 0 | 0 | 0 | $-\frac{5}{12}$ | $-\frac{5}{12}$ | $-\frac{5}{12}$ |

TABLE VII. (*Continued*).

| $l'_u l'_d$ $l_u l_d$ | 12 | 13 | 23 | 45 | 46 | 56 | 14 | 15 | 16 | 24 | 25 | 26 | 34 | 35 | 36 |
|---|---|---|---|---|---|---|---|---|---|---|---|---|---|---|---|
| $\rho S$ $\lambda S$ | 0 | $-3/4\sqrt{3}$ | $3/4\sqrt{3}$ | 0 | 0 | 0 | $5/12\sqrt{3}$ | $5/12\sqrt{3}$ | $5/12\sqrt{3}$ | $-5/12\sqrt{3}$ | $-5/12\sqrt{3}$ | $-5/12\sqrt{3}$ | 0 | 0 | 0 |
| $\rho S$ $\rho\rho$ | 0 | 0 | 0 | 0 | 0 | 0 | 0 | 0 | 0 | 0 | 0 | 0 | $-1/\sqrt{6}$ | $1/\sqrt{6}$ | 0 |
| $\rho S$ $\rho\lambda$ | 0 | 0 | 0 | 0 | 0 | 0 | 0 | 0 | 0 | 0 | 0 | 0 | $-1/3\sqrt{2}$ | $-1/3\sqrt{2}$ | $2/3\sqrt{2}$ |
| $\rho S$ $\lambda\rho$ | 0 | 0 | 0 | 0 | 0 | 0 | $1/3\sqrt{2}$ | $-1/3\sqrt{2}$ | 0 | $-1/3\sqrt{2}$ | $1/3\sqrt{2}$ | 0 | 0 | 0 | 0 |
| $\rho S$ $\lambda\lambda$ | 0 | 0 | 0 | 0 | 0 | 0 | $1/3\sqrt{6}$ | $1/3\sqrt{6}$ | $-2/3\sqrt{6}$ | $-1/3\sqrt{6}$ | $-1/3\sqrt{6}$ | $2/3\sqrt{6}$ | 0 | 0 | 0 |
| $\lambda S$ $\lambda S$ | $\frac{1}{4}$ | $-\frac{1}{2}$ | $-\frac{1}{2}$ | $\frac{1}{4}$ | $\frac{1}{4}$ | $\frac{1}{4}$ | $-\frac{5}{18}$ | $-\frac{5}{18}$ | $-\frac{5}{18}$ | $-\frac{5}{18}$ | $-\frac{5}{18}$ | $-\frac{5}{18}$ | $\frac{5}{36}$ | $\frac{5}{36}$ | $\frac{5}{36}$ |
| $\lambda S$ $\rho\rho$ | 0 | 0 | 0 | 0 | 0 | 0 | $1/3\sqrt{2}$ | $-1/3\sqrt{2}$ | 0 | $-1/3\sqrt{2}$ | $1/3\sqrt{2}$ | 0 | 0 | 0 | 0 |
| $\lambda S$ $\rho\lambda$ | 0 | 0 | 0 | 0 | 0 | 0 | $1/3\sqrt{6}$ | $1/3\sqrt{6}$ | $-2/3\sqrt{6}$ | $-1/3\sqrt{6}$ | $-1/3\sqrt{6}$ | $2/3\sqrt{6}$ | 0 | 0 | 0 |
| $\lambda S$ $\lambda\rho$ | 0 | 0 | 0 | 0 | 0 | 0 | $-2/3\sqrt{6}$ | $2/3\sqrt{6}$ | 0 | $-2/3\sqrt{6}$ | $2/3\sqrt{6}$ | 0 | $1/3\sqrt{6}$ | $-1/3\sqrt{6}$ | 0 |
| $\lambda S$ $\lambda\lambda$ | 0 | 0 | 0 | 0 | 0 | 0 | $-2/9\sqrt{2}$ | $-2/9\sqrt{2}$ | $4/9\sqrt{2}$ | $-2/9\sqrt{2}$ | $-2/9\sqrt{2}$ | $4/9\sqrt{2}$ | $1/9\sqrt{2}$ | $1/9\sqrt{2}$ | $-2/9\sqrt{2}$ |
| $\rho\rho$ $\rho\rho$ | $-\frac{3}{4}$ | 0 | 0 | $-\frac{3}{4}$ | 0 | 0 | 0 | 0 | 0 | 0 | 0 | 0 | 0 | 0 | $\frac{1}{4}$ |
| $\rho\rho$ $\rho\lambda$ | 0 | 0 | 0 | 0 | $-3/4\sqrt{3}$ | $3/4\sqrt{3}$ | 0 | 0 | 0 | 0 | 0 | 0 | $-1/4\sqrt{3}$ | $1/4\sqrt{3}$ | 0 |
| $\rho\rho$ $\lambda\rho$ | 0 | $-3/4\sqrt{3}$ | $3/4\sqrt{3}$ | 0 | 0 | 0 | 0 | 0 | $-1/4\sqrt{3}$ | 0 | 0 | $1/4\sqrt{3}$ | 0 | 0 | 0 |
| $\rho\rho$ $\lambda\lambda$ | 0 | 0 | 0 | 0 | 0 | 0 | $\frac{1}{12}$ | $-\frac{1}{12}$ | 0 | $-\frac{1}{12}$ | $\frac{1}{12}$ | 0 | 0 | 0 | 0 |
| $\rho\lambda$ $\rho\lambda$ | $-\frac{3}{4}$ | 0 | 0 | $\frac{1}{4}$ | $-\frac{1}{2}$ | $-\frac{1}{2}$ | 0 | 0 | 0 | 0 | 0 | 0 | $\frac{1}{6}$ | $\frac{1}{6}$ | $-\frac{1}{12}$ |
| $\rho\lambda$ $\lambda\rho$ | 0 | 0 | 0 | 0 | 0 | 0 | $\frac{1}{12}$ | $-\frac{1}{12}$ | 0 | $-\frac{1}{12}$ | $\frac{1}{12}$ | 0 | 0 | 0 | 0 |
| $\rho\lambda$ $\lambda\lambda$ | 0 | $-3/4\sqrt{3}$ | $3/4\sqrt{3}$ | 0 | 0 | 0 | $-1/6\sqrt{3}$ | $-1/6\sqrt{3}$ | $1/12\sqrt{3}$ | $1/6\sqrt{3}$ | $1/6\sqrt{3}$ | $-1/12\sqrt{3}$ | 0 | 0 | 0 |
| $\lambda\rho$ $\lambda\rho$ | $\frac{1}{4}$ | $-\frac{1}{2}$ | $-\frac{1}{2}$ | $-\frac{3}{4}$ | 0 | 0 | 0 | 0 | $\frac{1}{6}$ | 0 | 0 | $\frac{1}{6}$ | 0 | 0 | $-\frac{1}{12}$ |
| $\lambda\rho$ $\lambda\lambda$ | 0 | 0 | 0 | 0 | $-3/4\sqrt{3}$ | $3/4\sqrt{3}$ | $-1/6\sqrt{3}$ | $1/6\sqrt{3}$ | 0 | $-1/6\sqrt{3}$ | $1/6\sqrt{3}$ | 0 | $1/12\sqrt{3}$ | $-1/12\sqrt{3}$ | 0 |
| $\lambda\lambda$ $\lambda\lambda$ | $\frac{1}{4}$ | $-\frac{1}{2}$ | $-\frac{1}{2}$ | $\frac{1}{4}$ | $-\frac{1}{2}$ | $-\frac{1}{2}$ | $\frac{1}{9}$ | $\frac{1}{9}$ | $-\frac{1}{18}$ | $\frac{1}{9}$ | $\frac{1}{9}$ | $-\frac{1}{18}$ | $-\frac{1}{18}$ | $-\frac{1}{18}$ | $\frac{1}{36}$ |

TABLE VIII. Basic direct and exchange spatial matrix elements.

Hyperfine and $U$ potentials: $\Lambda_{ij}=\delta^3(\vec{r}_{ij})$

$$s=\alpha^3/(2\pi)^{3/2}$$
$$n_{(\mathrm{red})}=F^{-1}\sum_{ij}\xi_i\xi_j/[\tfrac{1}{3}(\beta_i^2+\beta_j^2)+\tfrac{1}{2}\alpha^2]^{3/2}$$
$$b_{ss(\mathrm{red})}=B$$
$$b_{sn(\mathrm{red})}=216^{3/2}\alpha^3F^{-1}\sum_{ij}\xi_i\xi_j/(99\alpha^4+42\alpha^2\beta_i^2+78\alpha^2\beta_j^2+20\beta_i^2\beta_j^2)^{3/2}$$
$$b_{nc(\mathrm{red})}=(\tfrac{3}{2})^{3/2}\alpha^3F^{-1}[\sum_i\xi_i/(\alpha^2+\tfrac{1}{3}\beta_i^2)^{3/2}]^2$$
$$b_{ni(\mathrm{red})}=n_{(\mathrm{red})}$$

Confinement potential: $\Lambda_{ij}=r_{ij}^2$

$$s=3/\alpha^2$$
$$n_{(\mathrm{red})}=2/3+\frac{\alpha^2}{2F}\sum_{ij}\xi_i\xi_j/(\tfrac{1}{2}\beta_i^2+\tfrac{1}{2}\beta_j^2)^{5/2}$$
$$b_{ss(\mathrm{red})}=B$$
$$b_{sn(\mathrm{red})}=5B/8+\frac{27^{13/6}}{16F}\alpha^5\sum_{ij}\xi_i\xi_j(12\alpha^2+9\beta_j^2+\beta_i^2)/g_{ij}^{5/2}$$
$$b_{nc(\mathrm{red})}=B/2+\frac{27^{13/6}}{4F}\alpha^5\sum_{ij}\xi_i\xi_j(6\alpha^2+\beta_i^2+\beta_j^2)/g_{ij}^{5/2}$$
$$b_{ni(\mathrm{red})}=27^{13/6}\alpha^5F^{-1}\sum_{ij}\xi_i\xi_j(\tfrac{3}{2}\alpha^2+\beta_i^2+\beta_j^2)/g_{ij}^{5/2}$$

$$\begin{bmatrix}b_{ss}\\ b_{sn}\\ b_{nc}\\ b_{ni}\end{bmatrix}\equiv\int d\tau_{126;435}(125;436)^*\begin{bmatrix}\Lambda_{12}\\ \Lambda_{16}\\ \Lambda_{14}\\ \Lambda_{56}\end{bmatrix}(126;435)\,. \quad \text{(E2)}$$

We list, in Table VIII, the expressions for these quantities appropriate to both choices of $\Lambda_{ij}$. In the table the subscript "(red)" (for reduced) indicates that the quantity in question has been divided by the corresponding value of $s$.

In order to evaluate the exchange overlap integral $B$, as well as the exchange matrix elements of $\Lambda_{ij}$, the following relations between the Jacobi coordinates of the two distinct clusterings (126;435) and (125;436) are needed:

$$\vec{\rho}_{125}=\vec{\rho}_{126}\,, \quad \text{(E3)}$$
$$\vec{\rho}_{436}=\vec{\rho}_{435}\,, \quad \text{(E4)}$$
$$\vec{\lambda}_{125}=+\frac{2}{\sqrt{6}}\vec{\mathrm{R}}_{126;435}+\tfrac{2}{3}\vec{\lambda}_{435}+\tfrac{1}{3}\vec{\lambda}_{126}\,, \quad \text{(E5)}$$
$$\vec{\lambda}_{436}=-\frac{2}{\sqrt{6}}\vec{\mathrm{R}}_{126;435}+\tfrac{1}{3}\vec{\lambda}_{435}+\tfrac{2}{3}\vec{\lambda}_{126}\,, \quad \text{(E6)}$$
$$\vec{\mathrm{R}}_{125;436}=\tfrac{1}{3}\vec{\mathrm{R}}_{126;435}-\frac{4}{3\sqrt{6}}(\vec{\lambda}_{435}-\vec{\lambda}_{126})\,. \quad \text{(E7)}$$

These relations lead to

$$B=27^{3/2}\alpha^3F^{-1}\sum_{ij}\xi_i\xi_jg_{ij}^{-3/2}\,, \quad \text{(E8)}$$

where

$$g_{ij}=9\alpha^4+\tfrac{15}{2}\alpha^2(\beta_i^2+\beta_j^2)+4\beta_i^2\beta_j^2 \quad \text{(E9)}$$

and to the results of Table IX for the "generating matrix elements." A complete table of spatial matrix elements is not provided, the expressions being simple but too unwieldy. Those not listed can be generated from those in the table by permutational methods, using the conventional transformation properties recorded in Appendix A.

## APPENDIX F: KINETIC-ENERGY MATRIX ELEMENTS

In the center-of-mass system one can easily show that

$$K\equiv-\frac{1}{2m}\sum_{i=1}^{6}\nabla_i^2$$
$$=-\frac{1}{2(\frac{3}{2}m)}(\nabla_{R_{126;453}})^2$$
$$-\frac{1}{2m}[(\nabla_{\rho_{126}})^2+(\nabla_{\lambda_{126}})^2+(\nabla_{\rho_{453}})^2+(\nabla_{\lambda_{453}})^2]\,. \quad \text{(F1)}$$

Note that for well-separated clusters one would expect the mass appropriate to the intercluster coordinate motion to be the reduced mass of the two-nucleon system, i.e., $M_N/2$. We see that the mass which appears naturally in a nonrelativistic treatment is $3m/2$, where $m$ is the quark mass. In the presence of strong binding one may therefore run into a conflict, in general, as indeed happens with mesons. However, in our case, since we use a constituent quark mass of 330 MeV, the discrepancy is small and, as long as there is not much kinetic energy in the intercluster coordinate, (F1) is compatible with both the quark picture and the two-nucleon-with-internal-kinetic-energy picture.

In evaluating kinetic-energy matrix elements it is useful to note that the kinetic operator is symmetric in all quark

TABLE IX. Generating spatial matrix elements. The notation is $\langle l_1 l_2 \mid \Lambda_{ij} \mid l_3 l_4 \rangle \equiv (l_1 l_2, l_3 l_4; ij)$, where $l_i$ are symmetry labels, $l_1$ and $l_3$ referring to $u$'s, $l_2$ and $l_4$ to $d$'s.

| | | |
|---|---|---|
| $(SS_{\rm I},SS_{\rm I};ij)=$ | $s$ | $ij=12,13,23$ |
| | $n$ | $ij=45,46,56$ |
| | | Otherwise |
| $(SS_{\rm I},SS_{\rm II};ij)=$ | $(b_{ss}+2b_{sn})/[(1+8B)]^{1/2}$ | $ij=12,13,23$ |
| | $(4b_{sn}+4b_{nc}+b_{ni})/3[(1+8B)]^{1/2}$ | $ij=45,46,56$ |
| | | Otherwise |
| $(SS_{\rm II},SS_{\rm II};ij)=$ | $(s+2n+2b_{ss}+12b_{sn}+8b_{nc}+2b_{ni})/3(1+8B)$ | $ij=12,13,23$ |
| | $(4s+5n+12b_{ss}+40b_{sn}+16b_{nc}+4b_{ni})/9(1+8B)$ | $ij=45,46,56$ |
| | | Otherwise |
| $(SS_{\rm I},S\rho_{\rm II};ij)=$ | $\pm 3(b_{ss}-b_{sn})/[6(1-B)]^{1/2}$ | $ij=46,56$ |
| | $\pm(2b_{nc}-b_{sn}-b_{ni})/[6(1-B)]^{1/2}$ | $ij=14,24,34$ $15,25,35$ |
| | 0 | Otherwise |
| $(SS_{\rm II},S\rho_{\rm II};ij)=$ | $\pm\dfrac{(s-n+2b_{ss}+3b_{sn}-4b_{nc}-b_{ni})}{[6(1+8B)(1-B)]^{1/2}}$ | $ij=46,56$ |
| | $\mp\dfrac{(s-n+3b_{ss}+b_{sn}-2b_{nc}-2b_{ni})}{3[6(1+8B)(1-B)]^{1/2}}$ | $ij=14,24,34$ $15,25,35$ |
| | 0 | Otherwise |
| $(SS_{\rm I},\rho\rho_{\rm II};ij)=$ | $\pm(b_{nc}+b_{ni}-2b_{sn})/2[(1-B)]^{1/2}$ | $ij=14,25$ $24,15$ |
| | 0 | Otherwise |
| $(SS_{\rm II},\rho\rho_{\rm II};ij)=$ | $\mp\dfrac{(2s-2n+6b_{ss}+2b_{sn}-7b_{nc}-b_{ni})}{6[(1+8B)(1-B)]^{1/2}}$ | $ij=14,25$ $24,15$ |
| | 0 | Otherwise |
| $(S\rho_{\rm II},S\rho_{\rm II};ij)=$ | $(s+2n-b_{ss}-4b_{nc}+2b_{ni})/3(1-B)$ | $ij=12,13,23$ |
| | $(n-b_{ni})/(1-B)$ | $ij=45$ |
| | $(s+n+2b_{ss}-6b_{sn}+2b_{nc})/2(1-B)$ | $ij=46,56$ |
| | $(3s+3n-2b_{ss}-2b_{sn}-2b_{nc})/6(1-B)$ | $ij=14,24,34$ $15,25,35$ |
| | $(s+2n-b_{ss}-b_{ni})/3(1-B)$ | $ij=16,26,36$ |
| $(S\rho_{\rm II},\rho S_{\rm II};ij)=$ | $\mp(2s-2n-3b_{ss}+2b_{sn}+2b_{nc}-b_{ni})/6(1-B)$ | $ij=14,25$ $24,15$ |
| | 0 | Otherwise |
| $(S\rho_{\rm II},\rho\rho_{\rm II};ij)=$ | $\pm(s-n-b_{ss}+2b_{nc}-b_{ni})/(1-B)\sqrt{6}$ | $ij=13,23$ |
| | $\pm(b_{ss}-2b_{sn}+b_{nc})/(1-B)\sqrt{6}$ | $ij=14,15$ $24,25$ |
| | $\pm(n-s+b_{ss}-b_{ni})/(1-B)\sqrt{6}$ | $ij=16,26$ |
| | 0 | Otherwise |
| $(\rho\rho_{\rm II},\rho\rho_{\rm II};ij)=$ | $(n-b_{ni})/(1-B)$ | $ij=12,45$ |
| | $(s+n+b_{ss}-4b_{sn}+b_{nc})/2(1-B)$ | $ij=14,15,24,25$ |
| | $(n-2b_{nc}+b_{ni})/(1-B)$ | $ij=36$ |
| | $(s+n-b_{ss}-b_{nc})/2(1-B)$ | Otherwise |

coordinates and in fact in the color, spin, and spatial sectors independently. Therefore it connects only substates with the same joint spin-color-space $S_3^u \times S_3^d$ symmetries. This means that the kinetic-energy matrix is diagonal, apart from mixing between states 1 (3) and 14 (15) in the spin-1 sector and states 1 (3) and 8 (9) in the spin-0 sector. All matrix elements can be expressed in terms of the direct and exchange matrix elements

$$\begin{bmatrix} k_D \\ k_0 \end{bmatrix} \equiv \int d\tau_{126;435}(126;435)^* K \begin{bmatrix} (126;435) \\ (125;436) \end{bmatrix} . \quad \text{(F2)}$$

For the intercluster wave function given in Appendix B one finds

$$k_D = \frac{3\alpha^2}{m} + \frac{F^{-1}}{2m} \sum_{ij} \xi_i \xi_j \beta_i^2 \beta_j^2 (\tfrac{1}{2}\beta_i^2 + \tfrac{1}{2}\beta_j^2)^{-5/2} , \quad \text{(F3)}$$

$$k_0 = \frac{5\alpha^2}{m} B - \frac{2\alpha^2}{m} b_{sn(\text{red})}^{\text{confinement}} + 27^{3/2}\alpha^3 \frac{F^{-1}}{m} \sum_{ij} \xi_i \xi_j \beta_j^2 g_{ij}^{-3/2} [1 - g_{ij}^{-1}(\tfrac{15}{2}\alpha^2\beta_j^2 + 4\beta_i^2\beta_j^2)] , \quad \text{(F4)}$$

where $B$, $F$, $b_{sn(\text{red})}^{\text{confinement}}$, and $g_{ij}$ are as defined in Appendices B and E.

In the spin-1 sector the nonzero matrix elements, in the nonorthogonal basis given in Appendix B, are

$$K_{ii} = \begin{cases} (k_D + 8k_0)/(1+8B), & i = 1,3 \\ k_D, & i = 14,15 \\ (k_D - k_0)(/1-B), & \text{otherwise} \end{cases} \quad \text{(F5)}$$

$$K_{1,14} = K_{3,15} = K_{14,1} = K_{15,3} = 3k_0/(1+8B)^{1/2} .$$

Similarly, in the spin-0 sector, the nonzero matrix elements, in the nonorthogonal basis, are

$$K_{ii} = \begin{cases} (k_D + 8k_0)/(1+8B), & i,j = 1,3 \\ k_D, & i,j = 8,9 \\ (k_D - k_0)/(1-B), & \text{otherwise} \end{cases} \quad \text{(F6)}$$

$$K_{1,8} = K_{8,1} = K_{3,9} = K_{9,3} = 3k_0/(1+8B)^{1/2} .$$

## APPENDIX G: THE "PHYSICAL" BASIS

In the text we listed the content of the $I=0$, $J=1$ and $I=1$, $J=0$ channels in terms of physical three-quark configurations, in the standard isospin notation. It is clear that such a description is most suited to systems in which the two three-quark clusters are sufficiently separated that their overlap is negligible, for it is in that limit that two permutational components of a fully antisymmetrized wave function having distinct partitionings of particles between the two clusters are independent, and in which the physical situation can be described by choosing one particular partition and antisymmetrizing only within clusters. Six-quark states are then unambiguously described in terms of pairs of totally antisymmetrized three-quark clusters. A similar description exists for the basis in which isospin is realized dynamically. Here one merely replaces "totally antisymmetrized" by "appropriately antisymmetrized," where appropriately is taken to mean "totally" if the cluster consists of identical particles and "in identical particles only" if it does not. In evaluating van der Waals and tensor matrix elements we will, in fact, be in the limit of small exchange overlap and so shall find it convenient to work in this basis, which we describe, for future reference, as the "physical" basis. As an example, the possible "appropriately antisymmetrized" states of a $u_1u_2d_4$ cluster (with maximum spin projection) in its (symmetric) spatial ground state are

$$\rho\uparrow_{124}8^{\lambda}_{124}, \lambda\uparrow_{124}8^{\rho}_{124}, \quad \lambda\uparrow_{124}A_{124}, \text{ and } S^{\frac{3}{2}}{}_{124}A_{124} .$$

## APPENDIX H: THE VAN DER WAALS INTERACTION

The long-range piece of the confinement potential

$$V_c = -\tfrac{1}{2} \sum_{i<j} k r_{ij}^2 \frac{\vec{\lambda}_i}{2} \cdot \frac{\vec{\lambda}_j}{2} \quad \text{(H1)}$$

when expanded in terms of the cluster Jacobi coordinates of Appendix B, turns out to contain terms of the form $\vec{\lambda}_{126} \cdot \vec{\lambda}_{453}$, etc., which couple the *np* ground state, labeled (126;453), directly to four colored $P$-wave excitations:

$$(\lambda\lambda\lambda\lambda\rho\rho) \equiv (126_\lambda;453_\lambda)(\chi^{\lambda}_{126}\chi^{\lambda}_{453})_S(8^{\rho}_{126} \circ 8^{\rho}_{453}) , \quad \text{(H2)}$$

etc. A few comments regarding the notation in (H2) are in order:

$$(126_\lambda;453_\lambda) = \frac{2\alpha^3}{\sqrt{3}} \vec{\lambda}_{126} \cdot \vec{\lambda}_{453} \phi(126)\phi(453)\Psi(\vec{R}_{126;453}) \quad \text{(H3)}$$

is the normalized $L=0$ combination of two $P$-wave clusters with $S_3^{126} \times S_3^{453}$ symmetry $(\lambda\lambda)$ and, in general, different variational parameters from the ground state, $(\chi^{\lambda}_{126}, \chi^{\lambda}_{453})_S$ the spin-$S$ combination of spin-$\frac{1}{2}$ clusters 126 and 453, and $(8^{\rho}_{126} \circ 8^{\rho}_{453})$ the color-singlet combination of the $8^{\rho}$ 126 and 453 color wave functions. Note that we are working now in the "physical basis," i.e., the basis of three-quark clusters antisymmetrized separately in their identical particles. Since the $S_3^{126} \times S_3^{453}$ symmetries of the *np* states in the spin and color sectors, in this representation, are $(\lambda\lambda)$ and $(AA)$, respectively, and since the confinement potential is spin independent, the ground state is coupled only to states with spin configuration $(\lambda\lambda)$. The available states are therefore those with symmetries $(\lambda\lambda\lambda\lambda\rho\rho)$, $(\lambda\rho\lambda\lambda\rho\lambda)$, $(\rho\lambda\lambda\lambda\lambda\rho)$, and $(\rho\rho\lambda\lambda\lambda\lambda)$, of which the state above is an example.

The energy shift of the ground state caused by the mixing of the color-octet $P$-wave state (H2) is given in second-order perturbation theory by

$$\Delta E=\frac{-|\langle(\lambda\lambda\lambda\lambda\rho\rho)|V_c|np\rangle|^2}{(E_{(\lambda\lambda\lambda\lambda\rho\rho)}-E_{np})} \tag{H4}$$

with similar contributions for the other three states. The squared transition matrix element appearing in (H4) for each of the four states is

$$\tfrac{1}{6}(3k/2\alpha^2)^2\frac{1}{FF'}\left[\sum_{i,j}\xi_i'\xi_j(\tfrac{1}{2}\beta_i'^2+\tfrac{1}{2}\beta_j^2)^{-3/2}\right]^2, \tag{H5}$$

where $\xi_i'$, $\beta_i'$ are the variational parameters for the intercluster wave function of the excited state, and $F,F'$ (as given in Appendix B) are the normalization factors for the ground-state and excited-state intercluster wave functions, respectively. In evaluating the energy denominator in (H4) we note that the radial suppression at the origin allows us to neglect the cross-cluster contribution of the short-range $U$ perturbation. Those of the hyperfine interaction, although small, are retained because they contribute to the splitting of the $S=0$ and $S=1$ channels. The resulting expression for the energy denominator is, in all cases,

$$\begin{aligned}&\tfrac{3}{2}\alpha^2(\tfrac{3}{2}k\alpha^{-2})\sum_{ij}\xi_i'\xi_j'(\tfrac{1}{2}\beta_i'^2+\tfrac{1}{2}\beta_j'^2)^{-5/2}F'^{-1}\\&+\begin{Bmatrix}-1\\+\frac{1}{3}\end{Bmatrix}\left[\frac{8\pi\alpha_s\alpha^3}{3(2\pi)^{3/2}m^2}\right]2^{3/2}\sum_{ij}\xi_i'\xi_j'\left[\frac{12\alpha^4+6\alpha^2(\beta_i'^2+\beta_j'^2)+7(\beta_i'^2+\beta_j'^2)^2}{(\alpha^2+\frac{2}{3}\beta_i'^2+\frac{2}{3}\beta_j'^2)^{7/2}}\right]\frac{1}{48F'}\\&+k_D(\beta_i',\xi_i')-k_D(\beta_i,\xi_i)+\frac{\alpha^2}{m}+\frac{3}{8}\left[\frac{8\pi\alpha_s\alpha^3}{3(2\pi)^{3/2}m^2}\right]-\tfrac{1}{3}(\tfrac{3}{2}k\alpha^{-2})+3\left[\frac{w\alpha^3}{(2\pi)^{3/2}}\right],\end{aligned} \tag{H6}$$

where the factors $-1$ and $+\frac{1}{3}$ multiplying the second summation are for the $S=0$ and 1 channels, respectively, the last three terms arise from in-cluster expectations of the hyperfine and confinement potentials, and $k_D(\beta_i',\xi_i')$, $k_D(\beta_i,\xi_i)$ are the direct kinetic-energy matrix elements given by (F3).

For $r\gtrsim 3$ fm these expressions simplify so that the total contribution to the potential from these four states may be expressed analytically as $-5$ MeV $(r/3\text{ fm})^{-2}$.

## APPENDIX I: THE TENSOR INTERACTIONS

The tensor piece of the hyperfine interaction is a $J=0$, $L=2$, $S=2$ operator. It is convenient to display it in the following recoupled form in which this fact is evident. Writing

$$H_T=\sum_{jk}H_T^{jk} \tag{I1}$$

with

$$H_T^{jk}=\hat{H}_T^{jk}\frac{\vec{\lambda}_j}{2}\cdot\frac{\vec{\lambda}_k}{2}\equiv\hat{H}_T^{jk}\Lambda_{jk}^c, \tag{I2}$$

we have

$$\hat{H}_T^{jk}=-\frac{3\alpha_s}{m^2}\sum_n(-1)^n(\vec{S}_j\vec{S}_k)_{(2,n)}\left[\frac{\vec{r}_{jk}\vec{r}_{jk}}{r_{jk}^5}\right]_{(2,-n)}, \tag{I3}$$

where $(\vec{S}_j\vec{S}_k)_{(2,n)}$ is the $S=2$, $S_z=n$ combination of $\vec{S}_j,\vec{S}_k$ and $(\vec{r}_{jk}\vec{r}_{jk}/r_{jk}^5)_{(2,-n)}$ is the $L=2$, $L_z=-n$ combination of $\vec{r}_{jk}/r_{jk}^{5/2}$, $\vec{r}_{jk}/r_{jk}^{5/2}$. The matrix elements of an operator of this form between states of definite $L,S$ are readily obtained by standard invariance methods.[29] For a state $|I\rangle$ with $L=2$ and spin $S'$ coupled to the initial $np$ ground state ($L=0$, $S=1$) one finds

$$\langle I|\hat{H}_T^{jk}|np\rangle=-\frac{3\alpha_s}{m^2}(-1)^{S'-1}[5(2S'+1)]^{1/2}W(1,0,S',2;1,2)(S'||(\vec{S}_j\vec{S}_k)_2||1)\left[L'=2\left|\left|\left[\frac{\vec{r}_{jk}\vec{r}_{jk}}{r_{jk}^5}\right]_2\right|\right|L=0\right], \tag{I4}$$

where $W(1,0,S',2;1,2)$ is the Racah coefficient (whose value is $1/\sqrt{15}$) and $(\,||\,||\,)$ denotes a reduced matrix element.

We begin by considering the admixture of an $np$ $D$-wave component into the $np$ ground state. Starting with $(uud)(ddu)$ clustering in the "physical basis" one can readily show that the correct jointly antisymmetrized state is proportional to the product of sums of cyclic permutations of $u$'s and $d$'s acting on any representatively labeled state, i.e.,

$$\Phi_L = N \sum_{\substack{\text{cyc} \\ 123}} \sum_{\substack{\text{cyc} \\ 456}} \{126;453\}_L \ , \tag{I5}$$

where $\{126;453\}_L$ is the spin, space, color configuration of two three-quark clusters 126 and 453 in proton and neutron states, respectively, with relative orbital angular momentum $L$. Since we neglect second-order exchange effects in our tensor matrix elements we can drop the exchange contribution to the normalization and set $N=\frac{1}{3}$. The tensor interaction between $\Phi_2$ and $\Phi_0$ then consists of 9 direct terms (which do not contribute to the $D$-wave mixing) and 72 exchange terms, 36 each involving single and double exchanges. Using the permutational symmetry of the full tensor interaction one can show that all single-exchange terms are identical, as are all double-exchange terms, so that

$$\langle \Phi_2 | H_T | \Phi_0 \rangle = 4\langle \{126;453\}_2 | H_T | \{125;643\}_0 \rangle + 4\langle \{126;453\}_2 | H_T | \{315;642\}_0 \rangle \ . \tag{I6}$$

We therefore require the two-body color, reduced spin, and reduced spatial matrix elements with both of these permutational structures. The results are listed in Table X. The form used for the intercluster $D$-wave wave function is

$$\Psi_{2m}(R) \sim \sum_i \xi_i' R^2 Y_{2m}(\Omega_R) \exp(-\beta_i'^2 R^2) \ . \tag{I7}$$

From these results one obtains for this tensor mixing matrix element

$$-\left[\frac{8\pi\alpha_s\alpha^3}{3(2\pi)^{3/2}m^2}\right]\frac{\sqrt{10\pi}}{12\alpha^3\sqrt{3}}(8b_{sdn}+8b_{nds}-b_{nc}+22b_{ni}) \ , \tag{I8}$$

using the notation previously given in Table X. The energy difference between the $np$ ground state and its $D$-wave excitation, neglecting exchange terms, comes solely from the kinetic energy of the intercluster coordinate and is given by the expression

$$\frac{7}{6m}\frac{\sum_{ij}\xi_i'\xi_j'\beta_i'^2\beta_j'^2(\frac{1}{2}\beta_i'^2+\frac{1}{2}\beta_j'^2)^{-9/2}}{\sum_{ij}\xi_i'\xi_j'(\frac{1}{2}\beta_i'^2+\frac{1}{2}\beta_j'^2)^{-7/2}} - \frac{1}{2m}\frac{\sum_{ij}\xi_i\xi_j\beta_i^2\beta_j^2(\frac{1}{2}\beta_i^2+\frac{1}{2}\beta_j^2)^{-5/2}}{\sum_{ij}\xi_i\xi_j(\frac{1}{2}\beta_i^2+\frac{1}{2}\beta_j^2)^{-3/2}} \ . \tag{I9}$$

The remaining states, which consist of colored clusters, mix directly into the ground state and are of three general types:

$$(P^M_{126}P^{M'}_{453};L_{\text{rel}}=0)_{L=2} \ ,$$
$$(P^M_{126}S_{453};L_{\text{rel}}=1)_{L=2} \text{ or } (S_{126}P^M_{453};L_{\text{rel}}=1)_{L=2} \ ,$$
$$(S_{126}S_{453};L_{\text{rel}}=2)_{L=2} \ ,$$

where we have used the notations $S_{126}$, $P^M_{126}$ to represent ground-state and $P$-wave excited-state 126 clusters, respectively ($M=\rho$ or $\lambda$), and the subscript $L=2$ means that the available orbital angular momentum is coupled to yield $L_{\text{tot}}=2$. In order to implement (I4) we need the corresponding reduced spin and spatial matrix elements. There are a large number of these but fortunately they are of diagonal (direct) permutational character and readily evaluated. The results are listed in Table XI. The color matrix elements can be obtained from Table V by interchanging the labels 3,6. The normalized wave functions for the various states are taken to be

$$(P_{126}P_{453};L_{\text{rel}}=0)_{(22)}=\frac{\alpha^2}{\pi^{3/4}}\rho_{126+}\rho_{453+}\phi(126)\phi(453)\frac{1}{(F_1')^{1/2}}\sum_i \xi_i' \exp[-\tfrac{1}{2}\beta_i'^2(R_{126;453})^2] \ , \tag{I10}$$

where $F_1' = \sum_{ij}\xi_i'\xi_j'(\frac{1}{2}\beta_i'^2+\frac{1}{2}\beta_j'^2)^{-3/2}$;

$$(P_{126}S_{453};L_{\text{rel}}=1)_{(22)}=\frac{\alpha}{\pi^{3/4}}\rho_{126+}R_{126;453+}\phi(126)\phi(453)\frac{1}{(F_2')^{1/2}}\sum_i \xi_i' \exp[-\tfrac{1}{2}\beta_i'^2(R_{126;453})^2] \ , \tag{I11}$$

where $F_2' = \sum_{ij}\xi_i'\xi_j'(\frac{1}{2}\beta_i'^2+\frac{1}{2}\beta_j'^2)^{-5/2}$; and

$$(S_{126}S_{453};L_{\text{rel}}=2)_{(22)}=\frac{2^{-1/2}}{\pi^{3/4}}(R_{126;453+})^2\phi(126)\phi(453)\frac{1}{(F_3')^{1/2}}\sum_i \xi_i' \exp[-\tfrac{1}{2}\beta_i'^2(R_{126;453})^2] \ , \tag{I12}$$

where $F_3' = \sum_{ij}\xi_i'\xi_j'(\frac{1}{2}\beta_i'^2+\frac{1}{2}\beta_j'^2)^{-7/2}$, where $v_+ = v_x + iv_y$ so that $-v_+/\sqrt{2}$ is the usual (11) spherical component of the vector $\vec{v}$, $\phi(126)$ and $\phi(453)$ are the 126 and 453 cluster ground states, as in Appendix E, and $\xi_i'$, $\beta_i'$ are variational parameters, allowed to vary independently in each of the three cases. The subscript (22) means that the state is the $L=2$, $L_z=2$ member of the $D$-wave multiplet. To complete the calculation we must enumerate the available states of each type in the "physical basis," use the results of Table XI in (I2) to obtain the transition matrix elements, and evaluate the required energy denominators, i.e., the energy splittings of each of these states relative to the $np$ ground state. In the usual approximation, in which we neglect exchange terms and intercluster expectations of short-range operators, the energy denominators all have a common form:

TABLE X. The spin, space, and color matrix elements for the *np* tensor *D*-wave mixing. The states are labeled by their cluster permutation symmetries, the subscripts being the particle content of the clusters. Some symbols appearing here are defined in the text of Appendix I. The remainder are

$$b_{ss}=0\ ,$$

$$b_{sdn}=\frac{1}{(F'_3F)^{1/2}}\sum_{ij}\xi'_i\xi_j\frac{48}{5}\frac{54^{3/2}}{\pi^{1/2}}\frac{\alpha^8(\alpha^2-2\beta_j^2/3)^2}{(99\alpha^4+78\alpha^2\beta_i'^2+42\alpha^2\beta_j^2+20\beta_i'^2\beta_j^2)^{5/2}G_{ij}}\ ,$$

$$b_{nds}=\frac{1}{(F'_3F)^{1/2}}\sum_{ij}\xi'_i\xi_j\frac{\sqrt{6}}{\sqrt{\pi}}\frac{8(54^2)}{15}\frac{\alpha^8(3\alpha^2+2\beta_j^2)^2}{(99\alpha^4+78\alpha^2\beta_j^2+42\alpha^2\beta_i'^2+20\beta_i'^2\beta_j^2)^{5/2}G_{ij}}\ ,$$

$$b_{nc}=\frac{1}{(F'_3F)^{1/2}}\sum_{ij}\xi'_i\xi_j\frac{\sqrt{3}}{20\sqrt{\pi}}\alpha^8/(\alpha^2+\beta_i'^2/3)^{5/2}(\alpha^2+\beta_j^2/3)^{1/2}G_{ij}\ ,$$

$$b_{ni}=\frac{1}{(F'_3F)^{1/2}}\sum_{ij}\xi'_i\xi_j\frac{4\sqrt{2}}{5\sqrt{\pi}}\alpha^3(\alpha^2/3+4\beta_j^2/9)^2/(\alpha^2+2(\beta_i'^2+\beta_j^2)/3)^{5/2}G_{ij}\ ,$$

where

$$G_{ij}=\alpha^4+\tfrac{5}{6}\alpha^2(\beta_i'^2+\beta_j^2)+\tfrac{4}{9}\beta_i'^2\beta_j^2\ .$$

Color:

$$\langle A_{126}A_{453}\mid\Lambda^c_{jk}\mid A_{125}A_{643}\rangle=\begin{cases}-\frac{1}{9} & jk=14,24,13,23\\ -\frac{4}{9} & jk=56\\ \frac{2}{9} & \text{Otherwise}\end{cases}$$

$$\langle A_{126}A_{453}\mid\Lambda^c_{jk}\mid A_{315}A_{642}\rangle=\begin{cases}\frac{1}{9} & jk=25,23,56,36\\ \frac{4}{9} & jk=14\\ -\frac{2}{9} & \text{Otherwise}\end{cases}$$

Spin:

$$(\lambda_{126}\lambda_{453}(S=1)||(\vec{S}_j\vec{S}_k)_2||\lambda_{125}\lambda_{643}(S=1))=\begin{cases}-2\sqrt{5}/9\sqrt{3} & jk=12\\ -\sqrt{5}/9\sqrt{3} & jk=56\\ \sqrt{5}/36\sqrt{3} & jk=34,35,36\\ -\sqrt{5}/18\sqrt{3} & jk=45,46,13,23\\ \sqrt{5}/9\sqrt{3} & \text{Otherwise}\end{cases}$$

$$(\lambda_{126}\lambda_{453}(S=1)||(\vec{S}_j\vec{S}_k)_2||\lambda_{315}\lambda_{642}(S=1))=\begin{cases}25\sqrt{5}/72\sqrt{3} & jk=14\\ -\sqrt{5}/18\sqrt{3} & jk=56,23\\ -5\sqrt{5}/36\sqrt{3} & jk=12,13,45,46\\ 5\sqrt{5}/72\sqrt{3} & \text{Otherwise}\end{cases}$$

Space:

$$(S_{126}S_{453}(L=2)||(\vec{r}_{jk}\vec{r}_{jk}/r_{jk}^5)_2||S_{125}S_{643}(L=0))=\begin{cases}b_{ni} & jk=56\\ b_{ss} & jk=12,34\\ b_{sdn} & jk=16,26,35,45\\ b_{nds} & jk=15,25,36,46\\ b_{nc} & jk=14,24,13,23\end{cases}$$

$$(S_{126}S_{453}(L=2)||(\vec{r}_{jk}\vec{r}_{jk}/r_{jk}^5)_2||S_{315}S_{642}(L=0))=\begin{cases}b_{ni} & jk=14\\ b_{ss} & jk=26,35\\ b_{sdn} & jk=12,16,34,45\\ b_{nds} & jk=24,46,13,15\\ b_{nc} & jk=23,25,36,56\end{cases}$$

TABLE XI. Reduced spin and spatial matrix elements of diagonal permutational structure for the tensor interaction. As all matrix elements are direct, we will suppress the cluster indices 126;453. Thus $(\rho\rho;0)_2 \equiv (P^{\rho}_{126}P^{\rho}_{453};L_{\rm rel}=0)_{L=2}$, etc., and $(\sigma\sigma'(S)) \equiv (\sigma_{126}\sigma'_{453}(S_{\rm tot}=S))$, $\sigma,\sigma'$ being cluster permutational symmetry labels. We list matrix elements only for the required cross-cluster values of $jk$ and only for configurations independent under cluster interchange.

Spin:

$$([SS(S)]||(\vec{S}_j\vec{S}_k)_2||[\lambda\lambda(1)]) = \begin{cases} \frac{1}{3}\kappa(S) & jk=36 \\ -\frac{1}{6}\kappa(S) & jk=13,23,46,56 \\ \frac{1}{12}\kappa(S) & jk=14,24,15,25 \end{cases}$$

where $\kappa(3)=1$
$\kappa(2)=0$
$\kappa(1)=-\sqrt{2}/3\sqrt{3}$

$$([S\lambda(S)]||(\vec{S}_j\vec{S}_k)_2||[\lambda\lambda(1)]) = \begin{cases} \kappa'(S)/6\sqrt{2} & jk=14,15,24,25,36 \\ -\kappa'(S)/12\sqrt{2} & jk=13,23 \\ -\kappa'(S)/3\sqrt{2} & jk=46,56 \end{cases}$$

where $\kappa'(2)=1$
$\kappa'(1)=\sqrt{5}/3\sqrt{3}$

$$([S\rho(S)]||(\vec{S}_j\vec{S}_k)_2||[\lambda\lambda(1)]) = \begin{cases} 0 & jk=13,23,36 \\ \mp 3\kappa'(S)/12\sqrt{2} & jk=\begin{cases}14,24\\15,25\end{cases} \\ \pm 3\kappa'(S)/6\sqrt{2} & jk=\begin{cases}46\\56\end{cases} \end{cases}$$

$$([\rho\rho(1)]||(\vec{S}_j\vec{S}_k)_2||[\lambda\lambda(1)]) = \begin{cases} \pm 5/6\sqrt{3} & jk=\begin{cases}14,25\\15,24\end{cases} \\ 0 & jk=13,23,46,56,36 \end{cases}$$

$$([\rho\lambda(1)]||(\vec{S}_j\vec{S}_k)_2||[\lambda\lambda(1)]) = \begin{cases} 0 & jk=36,46,56 \\ \mp\frac{5}{9} & jk=\begin{cases}14,15\\24,25\end{cases} \\ \pm\frac{5}{18} & jk=\begin{cases}46\\56\end{cases} \end{cases}$$

$$([\lambda\lambda(1)]||(\vec{S}_j\vec{S}_k)_2||[\lambda\lambda(1)]) = \begin{cases} 2\sqrt{5}/9\sqrt{3} & jk=14,24,15,25 \\ -\sqrt{5}/9\sqrt{3} & jk=13,23,46,56 \\ \sqrt{5}/18\sqrt{3} & jk=36 \end{cases}$$

Space:

$$((SS;2)_2||(\vec{r}_{jk}\vec{r}_{jk}/r_{jk}^5)_2||(SS;0)_0) = \frac{8}{15}\frac{\sqrt{2}}{\sqrt{\pi}}\frac{1}{(F'_3F)^{1/2}}\sum_{ij}\xi'_i\xi_j\frac{\alpha^5}{H_{ij}^{5/2}(\beta_i'^2+\beta_j^2)}$$

where $H_{ij}=\alpha^2+\frac{2}{3}(\beta_i'^2+\beta_j^2)$

$$((\rho S;1)_2||(\vec{r}_{jk}\vec{r}_{jk}/r_{jk}^5)_2||(SS;0)_0) = \begin{cases} \pm\tau & jk=\begin{cases}14,15,13\\24,25,23\end{cases} \\ 0 & jk=36,46,56 \end{cases}$$

TABLE XI. (*Continued*).

$$((\lambda S;1)_2||(\vec{r}_{jk}\vec{r}_{jk}/r_{jk}^5)_2||(SS;0)_0)= \begin{cases} \tau/\sqrt{3} & jk=14,15,13,24,25,23 \\ -2\tau/\sqrt{3} & jk=36,46,56 \end{cases}$$

$$\text{where } \tau=\frac{8}{15}\frac{\sqrt{2}}{\sqrt{\pi}}\frac{1}{(F_2'F)^{1/2}}\sum_{ij}\xi_i'\xi_j\frac{\alpha^4(\beta_i'^2+\beta_j^2)}{H_{ij}^{5/2}[\alpha^2+8(\beta_i'^2+\beta_j^2)/3]}$$

$$((\rho\rho;0)_2||(\vec{r}_{jk}\vec{r}_{jk}/r_{jk}^5)_2||(SS;0)_0)= \begin{cases} \pm\sigma & jk=\begin{cases}14,25\\15,24\end{cases} \\ 0 & jk=13,23,46,56,36 \end{cases}$$

$$((\lambda\rho;0)_2||(\vec{r}_{jk}\vec{r}_{jk}/r_{jk}^5)_2||(SS;0)_0)= \begin{cases} \pm\sigma/\sqrt{3} & jk=\begin{cases}14,24\\15,25\end{cases} \\ \mp 2\sigma/3 & jk=\begin{cases}46\\56\end{cases} \\ 0 & jk=13,23,63 \end{cases}$$

$$((\lambda\lambda;0)_2||(\vec{r}_{jk}\vec{r}_{jk}/r_{jk}^5)_2||(SS;0)_0)= \begin{cases} \sigma/3 & jk=14,24,15,25 \\ -2\sigma/3 & jk=13,23,46,56 \\ 4\sigma/3 & jk=36 \end{cases}$$

$$\text{where } \sigma=\frac{-2}{15}\frac{1}{\sqrt{\pi}}\frac{1}{(F_1'F)^{1/2}}\sum_{ij}\xi_i'\xi_j\frac{\alpha^3(\beta_i'^2+\beta_j^2)}{H_{ij}^{5/2}}$$

$$(\tfrac{3}{2}k\alpha^{-2})\frac{pF_n'^{-1}\alpha^2}{2}\sum_{ij}\xi_i'\xi_j'(\tfrac{1}{2}\beta_i'^2+\tfrac{1}{2}\beta_j'^2)^{-(p+2)/2}+\frac{pF_n'^{-1}}{6m}\sum_{ij}\xi_i'\xi_j'\beta_i'^2\beta_j'^2(\tfrac{1}{2}\beta_i'^2+\tfrac{1}{2}\beta_j'^2)^{-(p+2)/2}$$

$$-\frac{F^{-1}}{2m}\sum_{ij}\xi_i\xi_j\beta_i^2\beta_j^2(\tfrac{1}{2}\beta_i^2+\tfrac{1}{2}\beta_j^2)^{-5/2}+\left[\frac{8\pi\alpha_s\alpha^3}{3(2\pi)^{3/2}m^2}\right]a_1+(\tfrac{3}{2}k\alpha^{-2})a_2+\left[\frac{w\alpha^3}{(2\pi)^{3/2}}\right]a_3+C\,, \tag{I13}$$

where $C,p$ depend only on the type of spatial excitation:

$$p=7,\ C=0 \text{ for } (S_{126}S_{453};L_{\rm rel}=2)_{L=2}\,, \tag{I14}$$

$$p=5,\ C=\frac{\alpha^2}{2m} \text{ for } (S_{126}P_{453}^M;L_{\rm rel}=1)_{L=2} \text{ and } (P_{126}^M S_{453};L_{\rm rel}=1)_{L=2}\,, \tag{I15}$$

$$p=3,\ C=\frac{\alpha^2}{m} \text{ for } (P_{126}^M P_{453}^M;L_{\rm rel}=0)_{L=2}\,, \tag{I16}$$

$n=(p-1)/2$ and the $a_i$ depend on the particular state. Terms with coefficients $(\frac{3}{2}k\alpha^{-2})$ arise from the quadratic part of the confinement potential, those with $[8\pi\alpha_s\alpha^3/3(2\pi)^{3/2}m^2]$ from the in-cluster hyperfine potential, those with $[w\alpha^3/(2\pi)^{3/2}]$ from the in-cluster $U$ perturbations, and the remainder from the kinetic energy. The accessible states of each type and corresponding values of $a_i$ are listed in Table XII together with the squared transition matrix elements.

## APPENDIX J: THE HYBRID OPE-POTENTIAL PLUS QUARK-POTENTIAL MODEL

We consider the system of a neutron and proton, in the deuteron channel, interacting via a potential with tensor and central pieces, each of which has contributions from both modified OPE and residual quark interactions. Note that the quark-induced tensor interactions are small (roughly 0.1 MeV in binding) and so have little effect, though we have included them for completeness.

Recall that, because of the pseudoscalar nature of the pion, a nonrelativistic reduction of the OPE diagram leads to a potential[30]

$$V(r)=\frac{f^2}{m^2}\vec{\tau}_1\cdot\vec{\tau}_2(\vec{\sigma}_1\cdot\vec{\nabla})(\vec{\sigma}_2\cdot\vec{\nabla})\hat{V}(r)\ , \tag{J1}$$

where $m$ is the pion mass, $r=|\vec{r}_1-\vec{r}_2|$, $\hat{V}(r)=\exp(-mr)/r$ is the pion field, $f^2\equiv(g^2/4\pi)(m/2M)^2$ with $g$ the bare $\pi NN$ coupling ($g^2/4\pi\simeq 15$), $M$ is the nucleon mass, and $\sigma_i$ and $\tau_i$ are the spin and isospin operators, respectively, of the $i$th particle. Nucleons couple, not directly to the pion field, but to gradients thereof. The modification of OPE due to form-factor softening (FFS) is implemented in momentum space by inserting a factor $\exp(-q^2/6\beta^2)$ at each $NN\pi$ vertex, where $\beta$ is phenomenologically determined and has the value 420 MeV.[31] The resulting coordinate space potential is obtained by convoluting the Fourier transform of the pion propagator, $\exp(-mr)/r$, with that of the form factor squared. One obtains

$$\hat{V}_{\rm FFS}(r)=\frac{f^2}{2m^2}\frac{\exp(m^2/3\beta^2)}{r}[\exp(mr)\mathrm{Erfc}(m/\sqrt{3}\beta-\sqrt{3}\beta r/2)-\exp(mr)\mathrm{Erfc}(m/\sqrt{3}\beta+\sqrt{3}\beta r/2)]\ , \tag{J2}$$

where

$$\mathrm{Erfc}(x)=\frac{2}{\sqrt{\pi}}\int_t^\infty dt\exp(-t^2)$$

is the complement of the error function. The central and tensor potentials corresponding to $\hat{V}_{\rm FFS}$ are obtained by first rewriting $(\vec{\sigma}_1\cdot\vec{\nabla})(\vec{\sigma}_2\cdot\vec{\nabla})$ in a form which displays its scalar and tensor pieces

$$\tfrac{1}{3}\vec{\sigma}_1\cdot\vec{\sigma}_2\nabla^2+\tfrac{1}{3}[3(\vec{\sigma}_1\cdot\vec{\nabla})(\vec{\sigma}_2\cdot\vec{\nabla})-\vec{\sigma}_1\cdot\vec{\sigma}_2\nabla^2] \tag{J3}$$

and then acting with the appropriate derivatives on $V(r)$ to obtain

$$(\vec{\sigma}_1\cdot\vec{\nabla})(\vec{\sigma}_2\cdot\vec{\nabla})\hat{V}(r)=\tfrac{1}{3}[\vec{\sigma}_1\cdot\vec{\sigma}_2V_c(r)+S_{12}V_T(r)]\ , \tag{J4}$$

where

$$V_c(r)=\frac{d^2\hat{V}(r)}{dr^2}+\frac{2}{r}\frac{d}{dr}V(r)\ , \tag{J5}$$

$$V_T(r)=\frac{d^2\hat{V}(r)}{dr^2}-\frac{1}{r}\frac{d}{dr}\hat{V}(r)\ , \tag{J6}$$

$$S_{12}=3(\vec{\sigma}_1\cdot\hat{r})(\vec{\sigma}_2\cdot\hat{r})-\vec{\sigma}_1\cdot\vec{\sigma}_2\ . \tag{J7}$$

The short-range $1/r$ attraction of the OPE potential is tamed by FFS and turned into a repulsion of width 1 fm. This repulsion is, however, no more physical than the OPE attraction as the pion field should be suppressed (FS) inside the nucleons. This means that we must modify the pion-field term $\exp(-mr)/r$ in the convolution integral and we do so by multiplying it by the factor $[1-\exp(-\sigma^2r^2)]^n$. We refer to the resulting potential as "form-factor-softened field-suppressed" (FFSFS). Because of the convolution one cannot get an immediate grasp of the significance of the parameters $\sigma,n$ but the overall effect is to suppress both tensor and central components significantly at short distances. Variations of $\sigma,n$ produce some change in the character of the tensor and central potentials, especially below 0.7 fm, but such variations are overwhelmed by the strong repulsive core of the residual quark interactions, so that our results are not particularly sensitive to such variations so long as they still produce deviations from the OPE tail beginning at reasonable separations.

We have chosen $\sigma=1000$ MeV and $n=12$ which produces a $V_c$ and $V_T$ which join the OPE tail around 1.5 fm, as shown in Figs. 3 and 4 of the text. We present, for completeness, the expression for $V$ in the FFSFS case. The FFS case may be recovered by setting $n$ to zero:

$$\hat{V}(r)=\frac{f^2}{2m^2}\sum_{k=0}^{n}(-1)^k\binom{n}{k}\frac{\exp[m^2/3\beta^2K(k)]}{[K(k)]^{1/2}}\chi_k\ ,$$

where

$$\chi_k=\sum_{\pm}(\pm)\frac{1}{r}\exp[\mp mr/K(k)-k^2\sigma^2r^2/K(k)]\times\mathrm{Erfc}\left\{\frac{m}{[3K(k)\beta^2]^{1/2}}\mp\left[\frac{3\beta^2r^2}{4K(k)}\right]^{1/2}\right\}\ , \tag{J8}$$

where $K(k)=1+4k\sigma^2/3\beta^2$. Writing the wave function for the deuteron in the form

$$\Psi_{11}(r)=\frac{1}{r}u_S(r)\Phi_{11,0}+\frac{1}{r}u_D(r)\Phi_{11,2}\ , \tag{J9}$$

where $\Phi_{11,0},\Phi_{11,2}$ are the normalized $J,J_z=1,1$ combinations of $S=1$, $L=0$ and $S=1$, $L=2$ states, respectively, one obtains the following equations for $u_S,u_D$ (Ref. 32):

TABLE XII. Colored cluster states with nonzero transition tensor matrix elements and the state-dependent coefficients of the energy denominators. States are labeled by their space, spin, and color cluster permutational symmetries in the order $\text{space}_a$ $\text{space}_b$ $\text{spin}_a$ $\text{spin}_b$ $\text{color}_a$ $\text{color}_b$ with $a=126$ and $b=453$. The transition matrix elements are those between the state in question and the $np$ ground state with the configuration $(SS\lambda\lambda AA)$. Since the results are segregated according to spatial excitation type, we suppress the labels that indicate this explicitly. $S_{\text{tot}}$ is the spin of the state in question. $\hat{\rho}\equiv\lambda$, $\hat{\lambda}\equiv\rho$. We do not list the results for the cluster interchanged $L_{\text{rel}}=1$ states.

The $(S_{126}S_{453};L_{\text{rel}}=2)_{L=2}$ sector

| States | $S_{\text{tot}}$ | $a_1$ | $a_2$ | $a_3$ | Transition matrix element squared |
|---|---|---|---|---|---|
| $(SSMM'\hat{M}\hat{M}')$ | 1 | $\frac{3}{2}$ | $-1$ | 3 | $f$ |
| $(SSSM\rho\hat{M})$ | 2 | $\frac{11}{8}$ | $-1$ | 3 | $9f/8$ |
| | 1 | $\frac{11}{8}$ | $-1$ | 3 | $f/8$ |
| $(SSMS\hat{M}\rho)$ | 2 | $\frac{11}{8}$ | $-1$ | 3 | $9f/8$ |
| | 1 | $\frac{11}{8}$ | $-1$ | 3 | $f/8$ |
| $(SSSS\rho\rho)$ | 3 | $\frac{5}{4}$ | $-1$ | 3 | $63f/20$ |
| | 1 | $\frac{5}{4}$ | $-1$ | 3 | $f/10$ |

$$\text{where } f=\frac{8\pi}{15}\left[\frac{8\pi\alpha_s\alpha^3}{3(2\pi)^{3/2}m^2}\right]^2\left[\sum_{ij}\frac{\xi_i'\xi_j\alpha^2}{(F_3'F)^{1/2}(\beta_i'^2+\beta_j^2)H_{ij}^{5/2}}\right]^2$$

The $(P^M_{126}S_{453};L_{\text{rel}}=1)_{L=2}$ sector

| State | $S_{\text{tot}}$ | $a_1$ | $a_2$ | $a_3$ | Transition matrix element squared |
|---|---|---|---|---|---|
| $(MSSS\hat{M}\rho)$ | 3 | $\frac{41}{32}$ | $-\frac{2}{3}$ | $\frac{23}{8}$ | $63g/80$ |
| | 1 | $\frac{41}{32}$ | $-\frac{2}{3}$ | $\frac{23}{8}$ | $g/40$ |
| $(MSSM'\hat{M}\hat{M}')$ | 2 | $\frac{45}{32}$ | $-\frac{2}{3}$ | $\frac{23}{8}$ | $9g/32$ |
| | 1 | $\frac{45}{32}$ | $-\frac{2}{3}$ | $\frac{23}{8}$ | $g/32$ |
| $(\rho S\lambda S\lambda\rho)$ | 2 | $\frac{13}{16}$ | $-\frac{2}{3}$ | 0 | $9g/8$ |
| | 1 | $\frac{13}{16}$ | $-\frac{2}{3}$ | 0 | $g/8$ |
| $(\rho S\rho S\rho\rho)$ | 2 | $\frac{9}{8}$ | $-\frac{1}{3}$ | 0 | $9g/32$ |
| | 1 | $\frac{9}{8}$ | $-\frac{1}{3}$ | 0 | $g/32$ |
| $(\lambda S\rho S\lambda\rho)$ | 2 | $\frac{11}{8}$ | $-\frac{1}{3}$ | 0 | $9g/32$ |
| | 1 | $\frac{11}{8}$ | $-\frac{1}{3}$ | 0 | $g/32$ |
| $(\rho S\lambda M\lambda\hat{M})$ | 1 | $\frac{15}{16}$ | $-\frac{2}{3}$ | 0 | $g$ |
| $(\rho S\rho M\rho\hat{M})$ | 1 | $\frac{5}{4}$ | $-\frac{1}{3}$ | 0 | $g/4$ |
| $(\lambda S\rho M\lambda\hat{M})$ | 1 | $\frac{3}{2}$ | $-\frac{1}{3}$ | 0 | $g/4$ |

$$\text{where } g=\frac{81\pi}{8}\left[\frac{8\pi\alpha_s\alpha^3}{3(2\pi)^{3/2}m^2}\right]^2\tau^2\alpha^{-6}$$

$$\frac{d^2u_S}{dr^2}+M[E-V_c(r)]u_S-\sqrt{8}MV_T(r)u_D=0\,, \tag{J10}$$

$$\frac{d^2u_D}{dr^2}+M\left[E-\frac{6}{Mr^2}-V_c(r)+2V_T(r)\right]u_D-\sqrt{8}MV_T(r)u_S=0\,, \tag{J11}$$

where $V_C$ and $V_T$ are now the central and tensor pieces of the full quark plus FFSFS pion potential. We solve this system variationally using as variational wave functions the forms already employed in the quark calculation. (See Appendices B and I for $u_S$ and $u_D$, respectively.) This is, of course, not the ideal choice if one wishes to obtain $D$-state probabilities and quadrupole moments for the deute-

TABLE XII. (*Continued*).

The $(P^{M}_{126}P^{M'}_{453};L_{\rm rel}=0)_{L=2}$ sector

| States | $S_{\rm tot}$ | $a_1$ | $a_2$ | $a_3$ | Transition matrix element squared |
|---|---|---|---|---|---|
| $(MM'SS\hat{M}\hat{M}')$ | 3 | $\frac{21}{16}$ | $-\frac{1}{3}$ | $\frac{11}{4}$ | $63h/320$ |
| | 1 | $\frac{21}{16}$ | $-\frac{1}{3}$ | $\frac{11}{4}$ | $h/160$ |
| $(\rho\rho\rho\rho\rho\rho)$ | 1 | 1 | $\frac{1}{3}$ | $\frac{17}{4}$ | $h/16$ |
| $(\rho\lambda\rho\rho\rho\lambda)$ | 1 | $\frac{5}{4}$ | $\frac{1}{3}$ | $\frac{17}{4}$ | $h/16$ |
| $(\lambda\rho\rho\rho\lambda\rho)$ | 1 | $\frac{5}{4}$ | $\frac{1}{3}$ | $\frac{17}{4}$ | $h/16$ |
| $(\lambda\lambda\rho\rho\lambda\lambda)$ | 1 | $\frac{3}{2}$ | $\frac{1}{3}$ | $\frac{17}{4}$ | $h/16$ |
| $\left[\begin{bmatrix}\rho\rho\\ \lambda\rho\end{bmatrix}S\lambda\begin{bmatrix}\lambda\lambda\\ \rho\lambda\end{bmatrix}\right]$ | 2 | $\frac{27}{32}$ | $-\frac{1}{3}$ | $\frac{11}{4}$ | $9h/32$ |
| $\left[\begin{bmatrix}\rho\rho\\ \rho\lambda\end{bmatrix}\lambda S\begin{bmatrix}\lambda\lambda\\ \lambda\rho\end{bmatrix}\right]$ | 1 | $\frac{27}{32}$ | $-\frac{1}{3}$ | $\frac{11}{4}$ | $h/32$ |
| $\left[\begin{bmatrix}\rho\rho\\ \lambda\rho\end{bmatrix}S\rho\begin{bmatrix}\lambda\rho\\ \rho\rho\end{bmatrix}\right]$ | 2 | $\frac{37}{32}$ | 0 | $\frac{7}{2}$ | $9h/128$ |
| $\left[\begin{bmatrix}\rho\rho\\ \rho\lambda\end{bmatrix}\rho S\begin{bmatrix}\rho\lambda\\ \rho\rho\end{bmatrix}\right]$ | 1 | $\frac{37}{32}$ | 0 | $\frac{7}{2}$ | $h/128$ |
| $\left[\begin{bmatrix}\rho\lambda\\ \lambda\lambda\end{bmatrix}S\rho\begin{bmatrix}\lambda\lambda\\ \rho\lambda\end{bmatrix}\right]$ | 2 | $\frac{45}{32}$ | 0 | $\frac{7}{2}$ | $9h/128$ |
| $\left[\begin{bmatrix}\lambda\lambda\\ \lambda\rho\end{bmatrix}\rho S\begin{bmatrix}\lambda\rho\\ \lambda\lambda\end{bmatrix}\right]$ | 1 | $\frac{45}{32}$ | 0 | $\frac{7}{2}$ | $h/128$ |
| $\left[\rho\rho\begin{bmatrix}\lambda\rho\lambda\rho\\ \rho\lambda\rho\lambda\end{bmatrix}\right]$ | 1 | $\frac{11}{16}$ | 0 | $\frac{7}{2}$ | $h/4$ |
| $(\rho\lambda\lambda\rho\lambda\lambda)$ | 1 | $\frac{15}{16}$ | 0 | $\frac{7}{2}$ | $h/4$ |
| $(\lambda\rho\rho\lambda\lambda\lambda)$ | 1 | $\frac{15}{16}$ | 0 | $\frac{7}{2}$ | $h/4$ |
| $(\rho\rho\lambda\lambda\lambda\lambda)$ | 1 | $\frac{3}{8}$ | $-\frac{1}{3}$ | $\frac{11}{4}$ | $h$ |

where $h=\frac{5\pi}{3}\left[\frac{8\pi\alpha_s\alpha^3}{3(2\pi)^{3/2}m^2}\right]^2\sigma^2\alpha^{-6}$

ron since these wave functions fall off as Gaussians at large distances rather than exponentially, and such quantities are sensitive to the long-range behavior of the wave function. However, our aim here is not to produce a detailed phenomenology of the system but to illustrate the plausibility of the physical ideas discussed in the text. The results are quite reasonable in this context. The central portion of the FFSFS OPEP produces only small energy shifts, but the strong tensor coupling results in a roughly 2-MeV increase of the binding energy and a $D$-wave admixture, quadrupole moment and rms radius as given in Table III.

*Present address: Lawrence Berkeley Laboratory, Building 50A, University of California at Berkeley, Berkeley, California 94720.

[1]This study is more fully described in the Ph.D. thesis (Department of Physics, University of Toronto, 1983) of one of us (K.M.). A brief account of this work has already appeared in Kim Maltman and Nathan Isgur, Phys. Rev. Lett. 50, 1827 (1983).

[2]The model has been described in several places. For a pedagogical treatment, see Nathan Isgur, in *The New Aspects of Subnuclear Physics,* edited by A. Zichichi (Plenum, New York, 1980). For reports on the applications of the model see Refs. 3.

[3]Gabriel Karl, in *Proceedings of the XIXth International Conference on High Energy Physics,* edited by S. Homma, M. Kawaguchi, and H. Miyazawa (Physical Society of Japan, Tokyo, 1978), p. 135; O. W. Greenberg, Ann. Rev. Nucl. Part. Sci. 28, 327 (1978); A. J. G. Hey, in *Baryon 1980,* proceedings of the 4th International Conference on Baryon Resonances, Toronto, edited by N. Isgur (University of Toronto, Toronto, 1980), p. 223; Jonathan Rosner, in *Techniques and Concepts in High Energy Physics,* proceedings of a NATO Advanced Study Institute, St. Croix, 1980, edited by T. Ferbel (Plenum, New York, 1981), p. 1; Nathan Isgur, in *Particles and Fields—1981: Testing the Standard Model,* proceedings of the Meeting of the Division of Particles and Fields of the APS, Santa Cruz, California, edited by C. Heusch and W. T. Kirk (AIP, New York, 1982), p. 1.

[4]For a discussion of the $U$ perturbation see Ref. 2 and also K. C. Bowler *et al.*, Phys. Rev. Lett. 45, 97 (1980).

[5]For recent discussions, see L. J. Reinders, in *Baryon 1980* (Ref. 3), p. 203; F. E. Close and R. H. Dalitz, in *Proceedings of the Workshop on Low and Intermediate Energy Kaon-Nucleon Physics, Rome, 1980,* edited by E. Ferrari and G. Violini (Reidel, Dordrecht, 1981), p. 411; H. R. Fiebig and B. Schwesinger, Nucl. Phys. A393, 349 (1983); D. Gromes, Z. Phys. C 18, 249 (1983).

[6]The $\vec{\lambda}_i\cdot\vec{\lambda}_j$ confinement potential has a long history, beginning with Y. Nambu, in *Preludes in Theoretical Physics,* edited by A. de Shalit, H. Feshbach, and L. van Hove (North-Holland, Amsterdam, 1966), p. 133; and H. J. Lipkin, Phys. Lett. 45B, 267 (1973). In its modern form, especially as applied to multiquark systems, it may be traced from H. J. Lipkin, in *Common Problems in Low- and Medium-Energy Nuclear Physics,* proceedings of the NATO Advanced Study Institute, Banff, 1978, edited by B. Castel, B. Gouland, and F. C. Khanna (Plenum, New York, 1979), p. 173; R. S. Willey, Phys. Rev. D 18, 270 (1978); M. B. Gavela *et al.*, Phys. Lett. 79B, 459 (1979); and also Ref. 2.

[7]For a recent pedagogical discussion see O. W. Greenberg and H. J. Lipkin, Nucl. Phys. A370, 349 (1981). The literature on van der Waals—type forces can be traced through this paper, but see also M. B. Gavela *et al.*, Phys. Lett. 82B, 431 (1979); G. Feinberg and J. Sucher, Phys. Rev. D 20, 1717 (1979).

[8]Consider, for example, the simpler $qq\bar{q}\bar{q}$ system in an overall color singlet. In the $(qq)_6(\bar{q}\bar{q})_{\bar{6}}$ sector of the system the $qq$ force is "anticonfining" and would in isolation lead to a spectrum unbounded from below, but the overall potential in the $qq$ relative coordinate is confining (due to the other two interactions of each quark). See Ref. 23 for details. The $\vec{\lambda}_i\cdot\vec{\lambda}_j$ potential in fact often imitates more realistic (multibody) stringlike potentials in color-singlet states. For example, if any single quark (or antiquark) is pulled away from a multiquark system, it will feel a stringlike potential energy as it is separated from the cluster of remaining quarks. Analysis of such a situation shows that the resultant stringlike potential is in general the sum of many two-body potentials with opposite signs. Thus the existence of subpotentials which are "anticonfining" is probably not pathological: it merely corresponds to an artifact of the decomposition of the potential into color subunits. We are grateful to R. H. Dalitz and J. Paton for discussions of these points.

[9]H. J. Lipkin, Phys. Lett. 113B, 490 (1982).

[10]Jack Paton and Nathan Isgur, Phys. Lett. 124B, 247 (1983).

[11]Nathan Isgur and Gabriel Karl, Phys. Rev. D 20, 1191 (1979).

[12]S. Otsuki, R. Tamagaki, and W. Wada, Prog. Theor. Phys. 32, 220 (1964); R. Tamagaki, Rev. Mod. Phys. 39, 629 (1967).

[13]David A. Liberman, Phys. Rev. D 16, 1542 (1977).

[14]Carleton DeTar, Phys. Rev. D 17, 323 (1978).

[15]Both calculations were adiabatic and we have proved (along with others: see, e.g., Harvey in Ref. 21) that this is not a viable approximation. The DeTar calculation has other related difficulties: see Chun Wa Wong and Keh-Fei Liu, in *Topics in Nuclear Physics,* proceedings of the International Winter School in Nuclear Physics, Peking, 1980, edited by T. T. S. Kuo and S. S. M. Wong (Springer, Berlin, 1981), p. 1. In addition, both calculations failed to allow for configuration mixing: see Yu. F. Smirnov *et al.*, Yad. Fiz. 27, 860 (1978) [Sov. J. Nucl. Phys. 27, 456 (1978)]; V. G. Neudatchin, Yu. F. Smirnov, and Ryozo Tamagaki, Prog. Theor. Phys. 58, 1072 (1977); I. T. Obukhovsky *et al.*, Phys. Lett. 88B, 321 (1979); Yad. Fiz. 31, 516 (1980) [Sov. J. Nucl. Phys. 31, 269 (1980)]; K. Sink, J. Plum. Phys. 1, 212 (1983); see also Refs. 16, 19, 20, and 21.

[16]M. Harvey, Nucl. Phys. A352, 301 (1981); A352, 326 (1981).

[17]I. Bender and H. G. Dosch, Fortschr. Phys. 30, 633 (1982).

[18]C. S. Warke and R. Shanker, Phys. Rev. C 21, 2643 (1980).

[19]T. D. Babutsidze *et al.*, Yad Fiz. 33, 1406 (1981) [Sov. J. Nucl. Phys. 33, 754 (1981)]; H. Toki, Z. Phys. A294, 173 (1980); J. E. F. T. Ribiero, Z. Phys. C 5, 27 (1980); M. Oka and K. Yazaki, Phys. Lett. 90B, 41 (1980); D. Robson, *Progress in Particle and Nuclear Physics,* edited by D. Wilkinson (Pergamon, New York, 1982), Vol. 8, p. 257; M. Rosina *et al.*, *ibid.*, p. 417.

[20]M. Harvey, in Proceeding of the CAP Summer School on Progress in Nuclear Dynamics, Vancouver Island, 1982 (unpublished); Amand Faessler *et al.*, Phys. Lett. 112B, 201 (1982).

[21]S. A. Williams *et al.*, Phys. Rev. Lett. 49, 771 (1982). We have been unable to reconcile the conclusions of this paper with ours.

[22]J. A. Wheeler, Phys. Rev. 52, 1083 (1937); D. L. Hill and J. A. Wheeler, *ibid.* 89, 1102 (1953); J. J. Griffin and J. A. Wheeler, *ibid.* 108, 311 (1957).

[23]John Weinstein and Nathan Isgur, Phys. Rev. Lett. 48, 659 (1982); Phys. Rev. D 27, 588 (1983). The calculation described in these papers is the meson-meson version of the present calculation.

[24]K. Wildermuth and Y. C. Tang, *A Unified Theory of the Nucleus* (Academic, New York, 1977), Sec. 3.5c.

[25]M. Lacombe *et al.*, Phys. Rev. C 21, 861 (1980); K. Holinde and R. Machleidt, Nucl. Phys. A256, 479 (1976); R. V. Reid, Ann. Phys. (N.Y.) 50, 411 (1968).

[26]This is not to say that the short-range-part of $V_{NN}$ will not reflect many of the *characteristics* of meson exchange: the quark exchanges between our clusters give quantum-number exchanges identical to those which can be carried by nonexotic

mesons so that our picture is quite consistent with, for example, the usual systematics of two-body reaction mechanisms. We are grateful to P. Collins for illuminating comments on this issue.

[27]See, however, the comments in Appendix F.

[28]By a forbidden state we mean any nonantisymmetrized state which vanishes upon antisymmetrization. One can readily show that such states, in our cluster representation, must be localized at small intercluster separations. One must therefore check that the repulsive core in $V_{\text{eff}}$, which arises from our probabilistic interpretation of the intercluster wave function, is not a result of inadvertent inclusion of such forbidden states. It is indeed possible to verify that the core effects we have claimed are real. In a limited-parameter variational calculation, admixtures of forbidden states will be disfavored over admixtures of allowed configurations simply because the former do not alter the energy of the corresponding antisymmetrized state. The suppression we see in $\Psi$ as $r\to 0$ is strongly driven by the minimization so that we must only satisfy ourselves that the resulting variational state does not include a residual admixture of forbidden states. One check of this possibility is the fact that we see no evidence for parameter variations which leave the energy of our optimized state fixed, indicating that our intercluster wave function does not have the freedom to expand a forbidden state once it is optimized. These arguments thus show that our calculations tend to minimize the contributions of forbidden states. We can make this qualitative statement more quantitative by asking the following physical question which tests the accuracy of our explicit probabilistic interpretation of $\Psi$: what is the probability, in our optimized appropriately antisymmetrized state, to find a neutron and proton separated by some distance $r$, each with its three quarks localized at a point? The question is chosen to make a comparison of the actual probability and that obtained assuming a purely probabilisitic interpretation using only $|\Psi|^2$ as simple as possible. The answer in the approximation which gives rise to $V_{\text{eff}}$ is

$$9\frac{\alpha^{12}}{\pi^6}|\Psi(R_{126;453}=r)|^2 .$$

For a state dominated by the *np* component one can easily show that the corresponding exact answer is

$$9\frac{\alpha^{12}}{\pi^6}[\,|\Psi(R_{126;453}=r)|^2+\tfrac{1}{9}\Psi^*(R_{126;453}=r)\Psi_{\text{perm}}] ,$$

where

$$\Psi_{\text{perm}}\equiv\frac{\pi^3}{\alpha^6}[\,\Psi(R_{ijk,lmn})\phi(\rho_{ijk},\lambda_{ijk})\times\phi(\rho_{lmn},\lambda_{lmn})]\,|_{R_{126;453}=r,\rho_{126}=\lambda_{126}=\rho_{453}=\lambda_{453}=0}$$

with $ijk;lmn$ any partition of $1,\ldots,6$ representing one $(uud)$ and one $(ddu)$ cluster and distinct from 126;453. (This relatively simple form follows from the choice of pointlike neutron and proton configurations.) Thus we see that $\frac{1}{9}\Psi_{\text{perm}}/\Psi(R_{126;453}=r)$ is a physical measure of the error in our approximation. (The error, of course, may arise from both physical exchange effects and the possible presence of spurious forbidden states in $\Psi$.) The correction is straightforward to evaluate. It is 11% at $r=0$ fm, 8% at $r=0.25$ fm, 4% at $r=0.5$ fm, and $<1\%$ beyond $r=0.9$ fm. We see that the approximation is, in fact, justified, and that the repulsion is indeed physical in nature. We are grateful to M. Harvey for originally bringing to our attention the potential difficulties associated with forbidden states.

[29]See, for example, M. E. Rose, *Elementary Theory of Angular Momentum* (Wiley, New York, 1957).

[30]See, for example, J. Bjorken and S. Drell, *Relativistic Quantum Mechanics* (McGraw-Hill, New York, 1964), Chap. 10.

[31]Roman Koniuk and Nathan Isgur, Phys. Rev. Lett. 44, 845 (1980); Phys. Rev. D 21, 1868 (1980).

[32]See, for example, J. M. Eisenberg and W. Greiner, *Microscopic Theory of the Nucleus* (North-Holland, London, 1972).